Journal of Machine Learning Research 18 (2017) 1-34 Submitted 8/15; Revised 5/17; Published 11/17

Classification of Time Sequences using Graphs of Temporal Constraints

Mathieu Guillame-Bert MATHIEUG@ANDREW.CMU.EDU
Artur Dubrawski AWD@CS.CMU.EDU
Auton Lab, The Robotics Institute, School of Computer Science
Carnegie Mellon University, Pittsburgh, United States

Editor: Luc De Raedt

Abstract

We introduce two algorithms that learn to classify Symbolic and Scalar Time Sequences (SSTS); an extension of multivariate time series. An SSTS is a set of *events* and a set of *scalars*. An *event* is defined by a symbol and a time-stamp. A *scalar* is defined by a symbol and a function mapping a number for each possible time stamp of the data. The proposed algorithms rely on temporal patterns called Graph of Temporal Constraints (GTC). A GTC is a directed graph in which vertices express occurrences of specific events, and edges express temporal constraints between occurrences of pairs of events. Additionally, each vertex of a GTC can be augmented with numeric constraints on scalar values. We allow GTCs to be cyclic and/or disconnected. The first of the introduced algorithms extracts sets of co-dependent GTCs to be used in a voting mechanism. The second algorithm builds decision forest like representations where each node is a GTC. In both algorithms, extraction of GTCs and model building are interleaved. Both algorithms are closely related to each other and they exhibit complementary properties including complexity, performance, and interpretability. The main novelties of this work reside in direct building of the model and efficient learning of GTC structures. We explain the proposed algorithms and evaluate their performance against a diverse collection of 59 benchmark data sets. In these experiments, our algorithms come across as highly competitive and in most cases closely match or outperform state-of-the-art alternatives in terms of the computational speed while dominating in terms of the accuracy of classification of time sequences.

Keywords: classification, temporal data, sequential data, graphical constraint models, decision forests, symbolic and scalar time sequences, supervised learning

1. Introduction

Learning to classify from labeled training data is one of the flagship capabilities of machine learning. Classification is commonly used to model flat-table data, and in applications involving more complex representations such as (time) sequences or graphs, the information is typically "featurized" or "flattened" to fit the flat-table representation paradigm, so that standard classification algorithms can be readily applicable. In the case of symbolic time-stamped sequences, popular featurization techniques include representing time-since-previous-occurrence of an event, or computing frequency of occurrence (or other statistics or measures) over moving windows of time. Perhaps, a preferable alternative is to instead use classification algorithms capable of natively handling the temporal aspects of time-stamped sequences.

In this paper we introduce two parametric algorithms that belong to that specialized class. Both algorithms are designed to classify Symbolic and Scalar Time Sequences (SSTS); an expressive extension of the Time Series (TS) representation that remedies some of its limitations. In particular, SSTS extends the standard TS model by allowing non-uniform and asynchronous sampling, representing instantaneous sparse events as well as dense numeric sequences, and scaling well to highly-dimensional (multi-channel) application scenarios.

Both algorithms rely on a simple but expressive graphical pattern model for SSTS data called Graph of Temporal Constraints (GTC). A GTC is a conjunction of three types of conditions: (1) Existence of an event, (2) Constraint on the timestamp difference between two given events, and (3) Inequality constraints on the numerical values of a numerical time sequence at a time defined by a given event. Each GTC defines a Boolean function on an SSTS (or a TS).

The first algorithm presented in this paper, called the "GTC-Set", bootstraps training SSTSs and extracts fitting GTCs to form an ensemble model. Unlike methods relying on extracting all possible patterns and then applying a feature selection, our first algorithm directly build a final set co-dependent discriminant GTCs (all extracted GTC are used and no feature selection is applied). For this reason, the set of build GTCs is much smaller than the set of all possible GTCs. At the end of the learning process, each thusly extracted GTC is used as an individual "voter" in the classification procedure.

The second algorithm, called "GTC-DF", builds a bootstrapped decision forest where the condition in each decision node is defined as a GTC. Path of inference through each decision tree in this forest depends on whether a query STSS fulfills the constraints of the particular node's GTC or not. Here again, the GTC attached to each node is directly constructed on-the-fly instead of being selected from a pool of existing GTCs.

To assess performance of the GTC-Set and the GTC-DF algorithms, we evaluated them on a diverse collection of 59 temporal sequence classification data sets (all of them are available publicly), and compared against 13 alternative algorithms found in the literature. Results show that our algorithms are highly competitive and in most cases outperform state-of-the-art considered alternatives, both in terms of computing speed and accuracy of classification. Our algorithms are especially competitive for unaligned temporal sequence data, i.e. the data for which the value of an observation at a particular time t has no distinct predictive value, or in other words: classification performance does not depend on when we start observing the data. We also show how the users can interpret learned models based on the proposed GTC representation. Interpretability is often an important factor that determines practical usability of machine learning solutions in the real world, and our presented framework satisfies this requirement well.

This paper is structured as follows: Section 2 describes the SSTS representation and formalizes the classification problem for SSTS. Section 3 discusses related work and proposes a three-category taxonomy of time series classification algorithms. Sections 4 and 5 introduce the GTC representation and the GTC-Set/DF models. Section 6 presents and details our two classification algorithms. Section 7 summarizes results of empirical evaluations and comparisons, and Subsection 7.7 shows how a user can interpret a GTC-Set model. Concluding remarks wrap up the paper in Section 8.

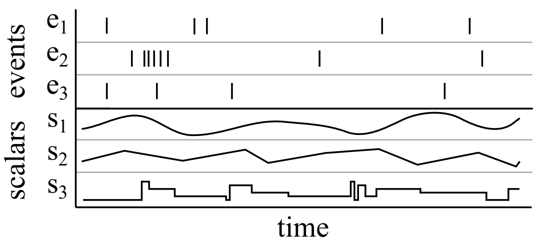

Figure 1: Example of an SSTS with three event symbols and three scalar variables.

2. Problem Definition

A Symbolic and Scalar Time Sequence (SSTS) is a temporal data set representation with a high power of expression. It is defined as follows:

Let $E = \{e_1, \ldots, e_n\}$ be a set of n distinct symbols called *event symbols*. Let $S = \{s_1, \ldots, s_m\}$ be a set of m distinct symbols called *scalar symbols*. An *event* is a tuple $\langle e_i, x\rangle$ where $x \in \mathbb{R}$ is a timestamp. A *scalar mapping* is a tuple $\langle s_i, f_i\rangle$ where f_i is a function $\mathbb{R} \mapsto \mathbb{R}; t \rightarrow v$ that maps each time-stamp t to a value v. Finally, a *symbolic and scalar time sequence* $d = \langle P, Q\rangle$ is a tuple where P is a set of events and Q is a set of scalar mapping. By convention, an event of type e_i is said to "happen" at time t if $\langle e_i, t\rangle \in P$, and the value of the scalar s_j at time t is $f_i(t)$ with $\langle s_i, f_i\rangle \in Q$. Figure 1 shows an example of SSTS. Note that an SSTS can contain several events with the same (event) symbol.

The SSTS classification problem is defined as follows: Given a set of labeled SSTSs and a set of unlabeled SSTSs drawn from the same underlying distribution, infer the labels of the unlabeled SSTSs.

3. Related Work

Published research into temporal data classification can be grouped into three categories: *distance based methods*, *flattening methods* and *model based methods*. This categorization does not take into account possible data pre-processing steps.

Distance based methods rely on a definition of a distance between pairs of time series, and the use of a distance-based classification algorithm (such as e.g. k-nearest neighbors). If the distance metric requires tuning of its parameters to optimize the data fit, the observations available for training are split into separate training and validation samples. Methods falling into this category include nearest neighbor and Euclidean distance (NN+ED) (Ding et al., 2008), NN+L1 (Ding et al., 2008), NN+Linf (Ding et al., 2008), DTW (Berndt and Clifford, 1994), LCSS (Vlachos et al., 2002), ERP (Chen et al., 2005), EDR (Chen and Ng, 2004), DISSIM (Frentzos et al., 2007), SWALE (Morse and Patel, 2007), TQUEST (Aßfalg et al., 2006).

Flattening methods work in two steps. Firstly, temporal data is transformed into a flat table in which each time series is decomposed into a set of features and then it is represented by a single row of the table. Secondly, a standard classification algorithm is applied to thusly prepared flat-table data (Random Forest (Breiman, 2001), SVM (Meyer et al., 2003), Artificial Neural Networks, or AdaBoost (Freund and Schapire, 2009) have all been used in this context). Types of features that are commonly used for flattening include basic statistics of the temporal data computed over moving time windows (mean, standard deviation, skewness, kurtosis, etc.), parameters prevalent in forecasting applications (trends, periodicity), and popular temporal signal projections (Fourier Transform, Wavelet Transforms, Singular Value Decomposition, etc.). Methods that rely on extracting a large amount of patterns from raw data followed by either applying feature selection and/or applying one of the classification algorithms to identify combinations of patterns that are effective on the task, fall into this category (Guillame-Bert and Dubrawski, 2014; Batal et al., 2012; Liu et al., 1998; Li et al., 2001). In this case, large amount of patterns are extracted according to user defined constraints (e.g. minimum support) and scores (e.g. F1), before being fed into a classifier. However, these methods are often slow because of the large amount of patterns to extract. And because discriminant power for classification does not always imply high score for a pattern, the methods may miss important patterns.

Finally, *direct-model-based methods* directly extract from data a model that contains temporal information. Examples of such methods include Rodríguez and Alonso (2004) and Deng et al. (2013) who have modified the decision forest framework (Breiman, 2001) to handle time series. In these approaches, conditions in the non-leaf nodes of the decision trees are of the form $f_i(t_1, t_2) < \alpha$ with $f_i(t_1, t_2)$ function computing a predefined statistic on all time series points between t_1 and t_2. For Rodríguez and Alonso (2004), $f_i(t_1, t_2)$ is the mean, standard deviation or the dynamic time warping distance to a template time series. For Deng et al. (2013), f is either the mean, standard deviation, or an estimation of the slope. Methods presented in Rodriguez et al., Deng et al. and Ye and Keogh (2009) do not fit the flattening paradigm because the features or conditions are determined at the time when the model is built instead of at a separate pre-processing stage. Inductive Logic Programming (Muggleton, 1991) (ILP) is a general framework that is capable to express many temporal patterns. Rodriguez et al. (2000) has shown an example of how to use ILP to classify time series. However, from our experience and because of their general nature, it is unclear how ILP solvers could learn efficiently temporal patterns containing time constraints which are not predefined by the users. The two algorithms proposed in this paper fall in this last category of methods.

One of the two proposed algorithms (GTC-Set) extracts large amount of GTC patterns (see definition in section 4), and use them with a simple voting mechanism (each active pattern casts a vote—the most represented class is predicted). This algorithm can be described trough the pattern-based classification framework described by Bringmann et al. Bringmann et al. (2011). In this framework, a pattern-based classification algorithm is divided into three parts: (1) The extraction of a pool of patterns, (2) the selection of a subset of patterns, and (3) the training of a classifier based on the patterns. The class of an algorithm is define by whether or not the labels are used in the stage (1) and (2) i.e. supervised or non-supervised pattern extraction and pattern selection: The main advantages of using labels in early stages is to "direct" the pattern extraction and selection, and to generate a smaller and more specialized (and hopefully more performant) set of patterns. On the other hand, not using labels in the first stage allows the use well studied of frequent pattern mining algorithms (e.g. frequent itemset mining (Agrawal and Srikant, 1994; Han et al., 2004), frequent sequence mining (Srikant and Agrawal, 1996; Zaki, 2001; Pei et al., 2001), frequent graph mining (Yan et al., 2008; Nowozin et al., 2007)). In this framework, the GTC-Set algorithm we propose is a "Model-dependent iterative mining" algorithm (i.e. the labels are used in the pattern extraction stage), and it does not contains a pattern selection nor training of a classifier stages: All extracted patterns are directly and independently used. Such simple application of extracted patterns is only possible because of the specific extraction of the GTC-Set algorithm. For example, directly and independently applying all patterns extracted from a frequent itemset mining algorithm would lead to poor results.

Supervised Descriptive Rule Discovery (Novak et al., 2009) (proposed as a unification of Contrast Set Mining (Bay and Pazzani, 2001), Emerging Pattern Mining (Dong and Li, 1999), and Subgroup Discovery (Klösgen, 1996)) is the supervised extraction of association rules from labeled transactional data sets for the purpose of user interpretation and data discovery. Rules are extracted to maximize a user defined interest score often measuring a lift-life measure or a statistical distance from a null-space model. Unlike pattern-based classification, these rules are not designed to be used for classification. In section 7.7, we discuss how to extract a small but representative subset of GTC patterns from set of patterns extracted by the GTC-Set algorithm. While being less performant for the classification task than the original set of patterns, the selected set of patterns aims to be easier to interpret by a user. The GTC-Set algorithm conjugated with pattern selection method can be seen as a solution to Supervised Descriptive Rule Discovery on SSTS. Interestingly, and contrary to most of the Supervised Descriptive Rule Discovery literature, the proposed method build an interpretable model from a classifier.

Unlike itemset mining, sequential mining allows for the definition and use of a relation of order in between items. This order is often used to represent the temporal sequence of the items: One item can be anterior, posterior or concurrent to another item. However, time distance is not taken into account by sequential mining, and in many dynamical systems, relations such as the time distance or the overlapping between items is discriminant.

In the literature, learning algorithms dealing with temporally discrete data (e.g. time point events) face the challenge of representing and extracting temporal constraints between pairs of time points. In most of the literature such constraints are represented with a subset C of $\mathbb{R}$: Given two data points with timestamps respectively t_1 and t_2, the constraint is satisfied if and only if $t_2 - t_1 \in C$.

This formulation has a high power of expression, but it can be prone to over-fitting given the potentially infinite number of candidate patterns and many available and applicable algorithms for pattern extraction are intractable. Solutions found in the literature rely on two principles: Constraining possible values of C, and/or defining an inexpensive to optimize score function on C. The simplest and the most popular solution is to require for the user to specify a small set of candidates for C (Mannila et al., 1997). Rodríguez and Alonso (2004) and Rodriguez et al. (2000) only consider segments of the form $[2^i, 2^j]$ where i and j are integers. Deng et al. (2013) consider a small number of randomly generated segments. Ye and Keogh (2009) show the use of a decision tree where node conditions are expressed as thresholds on the distance between the signal and a subset of a time series called "shapelet". During training, candidate shapelets are extracted from all possible subsets of training data, and pruning-based optimization is used to ensure tractability. Dousson and Vu Duong (1999) consider all segments. Recursively, the algorithm selects the segment $[a, b]$ that minimizes the surface $b - a$ while holding a user-defined minimum support. Guillame-Bert (2012) considers all possible unions from a large set of segments defined by the user $\{[ai+b, a(i+1)+b]\}_{i \in [m,n]}$. Recursively, the algorithm selects the set of segments that maximizes information gain. The maximization problem is solved approximately using a forward or backward gradient descent optimization. The resulting constraint is not necessarily a contiguous segment. Guillame-Bert and Dubrawski (2014) consider all combinations $[b_i, b_j]$ where $\{b_i\}$ are provided by the user, and i and j are selected to maximize information gain. All possible combinations of i and j can be evaluated thanks to an efficient specialized data encoding.

The algorithms proposed in this work rely on learning constraints of the type $[a, b]$ (a and b are not constrained). a and b are selected to maximize information gain. This is a strict improvement over Guillame-Bert and Dubrawski (2014). Efficient and exact, according to the information gain criterion, extraction of a and b is one of the main results of this work.

4. Graphs of Temporal Constraints

A Graph of Temporal Constraints (GTC) is a set of temporal constraints represented as a graph.

Definition 1 *A GTC is defined by a set of* tests $Q = \{q_1, \ldots, q_n\}$ *and a set of* constraints $C = \{c_1, \ldots, c_m\}$.

A test q_i is defined by an event symbol*, a positive or negative* flag*, and a (possibly empty) set of* scalar tests*. A q_i test with a positive flag is true at time t if an event with the given event symbol exists at time t, and if all its scalar tests are true at time t. A test with a negative flag is true if and only if the same test with a positive flag is impossible to satisfy.*

A scalar test *is an inequality constraint based on a scalar mapping value at a time t defined by the node. In this work, scalar tests are restricted to be inequalities between a single scalar mapping term and a threshold value.*

A constraint c_k *is defined by two tests q_i and q_j, a positive or negative flag, and $R \subset \mathbb{R}$ (a subset of the real numbers). A constraint with a positive flag is true if its both tests are true respectively at time t_i and t_j and if $t_j - t_i \in R$. A constraint with a negative flag is true if and only if the same constraint with a positive flag is false. In other words, a negative constraint $[a, b]$ is equivalent to the disjunctive constraint $]-\inf, a[\cup]b, +\inf[$. Additionally, we restrict GTC not to have conditions/edges starting from a negative test/node.*

This restriction is similar to the apriori constraint for association rule mining, and it guaranties that if built iteratively, the GTCs at successive steps have decreasing support.

A GTC can be seen as a directed graph were each vertex expresses the existential condition for an event (conditioned by a symbol), i.e. a test, and where each edge expresses a temporal constraint between the vertices it connects, i.e. a constraint. A GTC can contain undirected cycles and disconnected components. Fig. 2 shows two examples of GTCs.

Let us now introduce some aspects of notation used for describing GTCs. A GTC instance $\{k_i\}_{i \in 1,\ldots,n}$ assigns times k_i to each of the tests q_i of GTC A so that all tests and all constraints of A are true. By convention, $A(d)$ denotes the set of instances of A in an SSTS d. Note that different instances can partially overlap with each other. By convention, A is true in an SSTS d if d contains at least one instance of A, i.e. $|A(d)| > 0$. Trace $T(q_i, d)$ of the test q_i of A on the SSTS d is defined as the set of timestamps associated

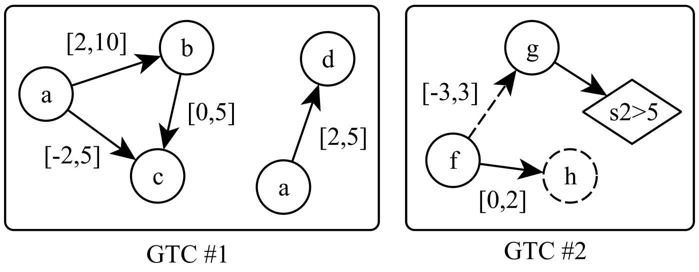

Figure 2: Two examples of GTCs. Dashed vertex (or edge) represents a vertex (or edge) with a negative flag. Diamond shapes represent scalar tests.

with the test q_i for any instances of A on d: $T(q_i, d) = \{k_i \mid \forall\{k_1, \ldots, k_i, \ldots, k_n\} \in A(d)\}$. Given a set of SSTS $D = \{d_1, \ldots, d_n\}$, $A(D)$ is the subset of SSTS for which A is true: $A(D) = \{d_i \mid d_i \in D \text{ with } |A(d_i)| > 0\}$. By convention, a GTC without tests is always true. Finally, given a set of SSTS D, the support of A is the fraction of SSTS where A is true: $supp(A) = |A(D)|/|D|$.

Testing the existence of a GTC in an SSTS (i.e. computing the existence of instances) can be done by (1) Extracting a set of spanning trees of the GTC (one tree for each of the GTCs disconnected components), (2) Independently matching each tree to the SSTS records while continuously, and (3) Checking any additional constraints that were not the part of the spanning trees. The cost of testing a GTC is polynomial with the number of events and exponential with the number of nodes. The smaller the surfaces of the temporal constraints between nodes, the less extensive the exploration, and the faster the GTC matching. However, in practice (cf. Experimental evaluation section below), the cost of testing GTCs is insignificant in comparison to the cost of learning these GTCs. It appears that because the constraints on the edges are selected to be discriminant, they tend to be restrictive and help in pruning large parts of the exploration space.

To the best of our knowledge, GTC is a novel representation, but it can be related to some existing temporal pattern representation frameworks. The closest are the Temporal Constraint Network (TCN) of Dechter (1991), the Chronicles of Dousson and Vu Duong (1999) and the Tita rules of Guillame-Bert (2012). TCN and Chronicles can be seen as reduced cases of GTCs in which tests and constraints do not have negative flags and in which there are no scalar tests. Tita rules allow node negation but do not allow undirected cycles or disjoint components.

5. Classification with GTCs

In this section, we introduce two SSTS classification models that use GTCs as their building blocks. The first model we call *GTC-Set*. A GTC-Set is an unstructured set of labeled (assigned to represent a particular unique class of STSS) GTCs. Given an unlabeled SSTS d, the predicted label for d is the most common label among all of the GTCs that are true on d. Note that this model would perform poorly if it were to contain all possible GTCs (even with a support constraint). Figure 3 shows an example of a GTC-Set.

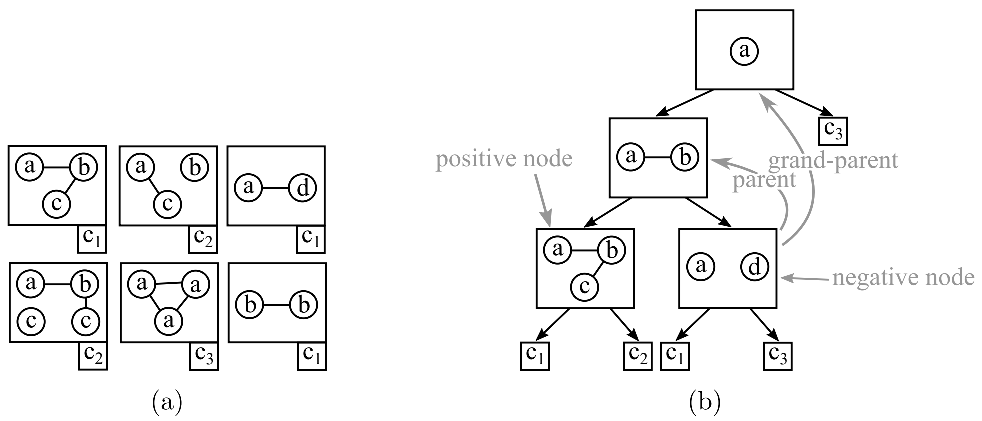

Figure 3: Examples of a GTC-Set (a) and a tree in a GTC-DF (b). Class labels in the leaf nodes are denoted with c_i.

The second model we call *GTC Decision Forest* (GTC-DF). A GTC-DF is a set of decision trees where each non-leaf node is associated with a particular GTC and it has two children. Additionally, the GTC attached to a decision tree node is constrained to be directly derived from the GTC of the parent node if connected by a positive decision tree branch, and from the grandparent node otherwise. This constraint is important and it will be discussed and justified in the next section. When applying a GTC-DF to classify a query in the form of a STSS, the decision trees are independently traversed in a familiar way. Upon arrival in a node, its associated GTC is tested for fitness to the data and the result of this test determines the direction of further traversal. As in the original decision forest algorithm (Breiman, 2001), class label distributions are agglomerated across the final active leaf nodes of each component tree, in order to obtain the joint prediction. Figure 3 shows an example of a tree in a GTC-DF.

Independence of components in GTC-Sets makes these models somewhat easier to interpret by the users than GTC Decision Forests because each of them can be considered individually. Conversely, interpretation of a GTC Decision Forest model, as well as its inference process in response to a particular query, requires consideration of GTCs corresponding to the subsequent nodes in each tree.

6. Learning Temporal Patterns

We introduce two algorithms to respectively extract GTC-Sets and GTC-DFs from a set of labeled SSTS instances. Both algorithms share the same sub-routines but differ in the structure of their main loops and therefore in the structure of the extracted GTCs. These algorithms can be seen as complementary. Experimentation shows that extracting GTC-DF is on average 40% faster, and it yields less complex models which typically perform slightly better when compared to GTC-Set models obtained from the same data (cf. Section 7.6). On the other hand, GTC-Sets allow easier interpretation of the results and the models themselves by the users (Section 7.7).

Both algorithms build GTCs by recursively applying constructive operations. In the process, selection of the next operation to apply is guided by maximizing the local information gain. This section presents GTC building operations, defines the concept of information gain of an operation, presents how to efficiently identify the operation with the highest information gain, and details the main loops of the two algorithms. Our proposed solution to how to efficiently extract optimal temporal constraints for the edges in GTCs is one of the main novelties of this work.

6.1 Constructive Operations on GTCs

Constructive operations on a GTC include:
O1: Addition of a new test (i.e. addition of a vertex),
O2: Addition of a constraint between two existing tests (i.e. addition of an edge),
O3: Addition of a scalar test to an existing test,
O4: Addition of a new test and addition of a constraint between this test and an already existing test.

Each operation requires specific parameters. O1 requires an event symbol and a positive/negative flag. O2 requires two existing tests, a flag and a subset of $\mathbb{R}$. O3 requires an existing test and a scalar test defined by a scalar symbol, a threshold value and an inequality direction ($<$ or $\geq$). O4 requires a combination of arguments of O1 and O2. Note that, because of the threshold value of the scalar test in O3, and because the need for a subset of $\mathbb{R}$ in O2 and O4, these operations have an infinite number of possible parameter values. Operation O4 is equivalent to operations 1 and 2 combined. We justify its existence later.

Both proposed algorithms require for the set of positive SSTS according to a GTC to be monotone decreasing when applying operations: Given a set D of SSTSs, a GTC A, an operation O and B the result of O on A. Algorithms require for the set of positive SSTSs according to B to be contained in the set of positive SSTSs according to A i.e. $B(D) \subset A(D)$. This implies that each operation reduces (albeit not strictly) the support of the GTC it is applied to. For this reason, operations O2-O4 cannot be applied on negative nodes.

The result of the negation of an operation O on a GTC A is a GTC B' such that $\forall d \in D, A(d) \Rightarrow (B(d) \Leftrightarrow \neg B'(d))$ and $\neg A(d) \Rightarrow (\neg B(d) \wedge \neg B'(d))$, where B is the result of O on A. Note: $\Leftrightarrow$ and $\neg$ are respectively the logical equivalence and logical negation. Except for trivial cases, the GTC resulting from the negation of an operation is more complex than the result of the operation. In the case of fully connected GTCs, the size of the GTC resulting from the negative operation is twice the size of the result from the direct operation. Instead, we define the approximate result of the negation of an operation. This approximation is not exact but it provides reasonable results as presented in Section 7.

Whether to use or not the approximate negation is the main difference between the two proposed algorithms. Figure 4 illustrates these operations and their associated approximate negations. Adding a constraint to a test with a negative flag would violate the support reduction property and it is therefore forbidden. The goal of O4 is to allow creating a connected test with a negative flag without violating the support reduction requirement.

As a simple example, consider the four GTCs shown in figure 5a. B is the result of an operation of type $O4$ on A. B' is the result of the negation of this operation. B'' is the

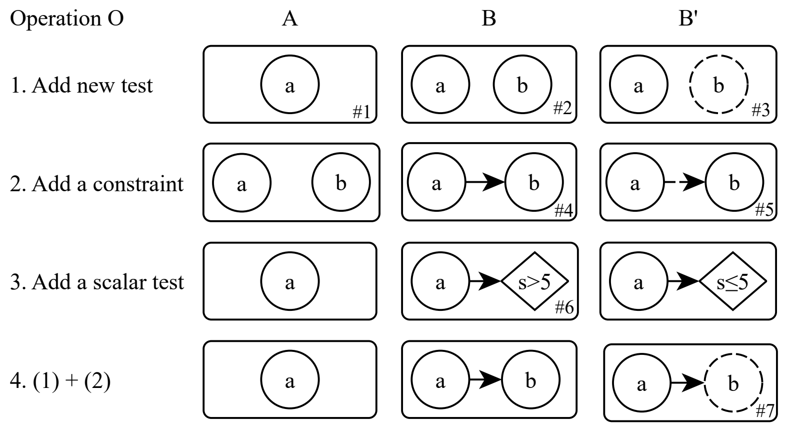

Figure 4: Illustration of the constructive operations on GTCs. Each row of graphs represents a specific operation. Column A represents the initial GTC. Column B shows the result of executing the particular operation on the initial GTC. Column B' depicts the result of the approximate negation of the operation. Dashed nodes and edges represent respectively tests and constraints with negative flags. Diamonds represent scalar tests. Description of the GTCs: #1: An event of type a is present. #2: An event of type a and an event of type b are present. #3: An event of type a is present, but no event of type b is present. #4: An event of type a and an event of type b are present, and they satisfy the constraint of the edge. #5: An event of type a and an event of type b are present, and they satisfy the complementary constraint of the edge. #6: An event of type a is present at time t such that the scalar s value is greater than 5 at time t. #7: An event of type a is present at time t_a such that there is no event b at time t_b such that t_a and t_b satisfy the constraint.

approximate result of the negation of this operation. A expresses that "There is an event a followed by an event b between 0 and 2 time units". B expresses that "There is an event a followed by an event b between 0 and 2 time units, itself followed by an event c between 1 and 3 time units". B' expresses that "There is an event a followed by an event b between 0 and 2 time units, but there is not an event a followed by an event b between 0 and 2 time units, itself followed by an event c between 1 and 3 time units". B'' expresses that "There is an event a followed by an event b between 0 and 2 time units, itself not followed by an event c between 1 and 3 time units". Figure 5b shows an SSTS B'' is true but where B' is not.

6.2 Information Gain Maximization

Both of the proposed GTC extraction algorithms are driven by the information gain maximization criterion. We define entropy H of a set of labeled SSTS D as the entropy of the

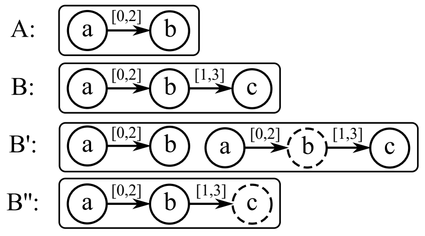

(a) Suppose a GTC A. B is the result of an operation of type $O4$ on A. B' is the result of the negation of this operation. B'' is the approximate result of the negation of this operation.

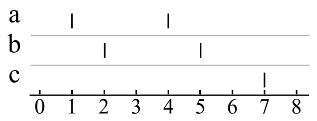

(b) Example of SSTS with B' false but B'' true.

Figure 5: Illustration of the negation and the approximate negation of an operation.

distribution of their labels

$$H(D) = \sum_i -p_i(D) \log p_i(D)$$

, with $p_i(D)$ representing the relative frequency of label i in D. Additionally, we assert $0 \log 0 = 0$.

Given a set of SSTSs $D = d_1, \dots, d_n$, a GTC A such that A is true for all d_i, and an operation O, if B is the result of O on A, then information gain IG of the operation O on A can be defined as

$$IG = H(D) - \frac{|B(D)|}{|D|} H(B(D)) - \frac{|D \setminus B(D)|}{|D|} H(D \setminus B(D))$$

, where $H(D)$ is commonly called the initial (prior) entropy, and the rest of the right hand side of the formula is the weighed final (posterior) entropy.

During the training stage, given a GTC A, both algorithms rely on finding such constructive operation and its parameters that maximize the information gain. Except for operation O1, testing and evaluating the information gain over the range of possible parameter values is in most cases infeasible because of the infinite number of tests it might involve. We propose a solution based on the following four considerations: (1) Instead of considering all subsets of $\mathbb{R}$ (operations O2 and O3), we only consider contiguous segments of $\mathbb{R}$; (2) Since each finite data set consists of a finite number of SSTSs, and each SSTS is composed of a finite number of events, there is only a finite number of parameter values that need to be considered; (3) The procedure of extracting a plausible threshold for an operation O3, and the corresponding segments of $\mathbb{R}$, can be optimized for computational speed with an appropriate algorithm and an appropriate internal data structure; and (4) Random sampling can be used as an option to further speed up the extraction of the optimum threshold and the optimum segments of $\mathbb{R}$.

The next two subsections show how to build decision forests and sets of GTCs models using information gain maximization. Subsection 6.5 shows how to compute efficiently the threshold of operation O3 that maximize their information gain. Subsection 6.6 shows how to compute efficiently the segment of R that maximize their information gain for operations O2 and O4.

6.3 Learning Decision Trees and Forests of GTCs

We build decision trees and forests of GTCs similarly to how standard decision trees and forests are built (Quinlan, 1993; Breiman, 2001). The two differences are that: (1) Each decision node of a GTC tree is assigned a GTC instead of a single threshold condition on a single data feature as it is the case of the standard model; and (2) The structure of a GTC representing a node of a GTC tree is heavily constrained by the structure of the GTCs of its parent and grand-parent nodes.

The algorithm for training a GTC tree starts with a single empty GTC and it looks for the operation on it that yields the highest information gain. This operation is then applied, and the resulting GTC is used to define the root node constraint. The root node constraint is used to split the training SSTSs into two complementary subsets. The same procedure is further recursively applied to these subsets and additional nodes are appended to the tree until a stopping criterion is met. The GTC of a positive node of the decision tree will be derived by applying a single operation on the GTC attached to its parent. The GTC of a negative node of the decision tree will be derived by applying a single operation on the GTC attached to its grand-parent. This restriction has three benefits: (1) Search space for the new GTC is limited and therefore fast to explore. (2) The new GTC is constrained and therefore the risk for it to over-fit is mitigated. (3) GTCs of an arbitrary complexity can still be derived. A GTC Decision Forest (GTC-DF) can be obtained by bootstrapping data for GTC decision tree learning from the training set of SSTSs. Note that we typically also bootstrap the GTC-Set models and in fact use ensembles of GTC-Sets, cf. Algorithm 2. Pseudocode in Algorithm 1 provides details.

Algorithm 1: Extraction of a GTC decision forest from data.

```
input  : $D$: A set of SSTSs
         $b$: The number of bootstrap iterations (e.g. 20)
         $l$: The minimum number of times a GTC is used (e.g. 5)
output: $M$: The set of extracted labeled GTCs
Algorithm
    for $i \leftarrow 1$ to $b$ do
        $A \leftarrow$ an empty GTC
        recursive_build($D, A$)
Subroutine recursive_build($D$,reference to $A$)
    $M \leftarrow M \cup A$
    if $|A(D)| < l$ then
        $label(A) \leftarrow$ most frequent class in $D$ with $A$ true
        return
    $o \leftarrow$ find the operation on $A$ with the highest information gain
    $B_2 \leftarrow A$
    $A \leftarrow$ result of $O$ on $A$
    $B_1 \leftarrow A$
    set $B_1$ and $B_2$ to be respectively the positive and negative children of $A$
    recursive_build($B_1(D), B_1$)
    recursive_build($D \setminus B_2(D), B_2$)
```

6.4 Learning Sets of GTCs

This sub-section introduces the algorithm to extract a GTC set from data. This algorithm starts with a single empty GTC A and looks for the operation with the maximum information gain to extend its structure. This operation and the approximate negation of it are applied to the GTC A to create two new GTCs, respectively B_1 and B_2. A is then removed. The same process is next recursively applied to both B_1 and B_2 until a stopping criterion is met. Finally, each remaining (i.e. non removed) GTC is assigned to the most common class of the SSTS where it is true. Note that because of the approximated negation $B_1(D)$ and $B_2(D)$ are not necessary disjoint (the last line of the Algorithm 2).

Algorithm 2: Extraction of a GTC set.

```
input  : $D$: A set of SSTSs
         $b$: The number of bootstrap iterations to execute (e.g. 20)
         $l$: The minimum number of times a GTC is used (e.g. 5)
output: $M$: The set of extracted labeled GTCs
Algorithm
    $A \leftarrow$ an empty GTC
    for $i \leftarrow 1$ to $b$ do
        $M \leftarrow M \cup$ recursive_build($D, A$)

Subroutine recursive_build($D$,$A$)
    if $|D(A)| < l$ then
        $label(A) \leftarrow$ most frequent class in $D$ with $A$ true
        return $A$
    $o_1 \leftarrow$ find the operation on $A$ with the highest information gain
    $o_2 \leftarrow$ approximate negation of $o_1$
    $B_1 \leftarrow$ result of $o_1$ on $A$
    $B_2 \leftarrow$ result of $o_2$ on $A$
    return recursive_build($B_1(D), B_1$) $\cup$ recursive_build($B_2(D), B_2$) // Note that it
        is not required nor expected that $B_1(D) \cap B2(D) = \emptyset$
```

6.5 Finding the Optimal Scalar Tests

A scalar test is defined by an existing test q_i, a scalar symbol s_j, a threshold value α and the direction of inequality ($<$ or $\geq$). The problem of finding the optimal threshold value is different but related to the problem of finding the optimal threshold in the decision tree learning algorithm C4.5 (Quinlan, 1993). Unlike C4.5, our algorithms need to consider several scalar values for each observation/SSTS: one scalar value for each GTC instance on a given SSTS.

To identify the optimal scalar test, the algorithm considers all possible existing tests q_i with a positive flag, every scalar symbol s_j, and both inequality directions $<$ and $\geq$. For each of these values, the algorithm computes the optimal threshold value α as follows. Consider a GTC A, the set of training SSTS $D = \{d_i\}_{1..n}$, the scalar symbol s_j, the existing test q_i of A, and the inequality direction $<$ or $\geq$. We first compute a $n \times 2$ matrix L defined as follows:

$$L[j,1] = \left\{ \begin{array}{ll} \min(\{s_j(x) | \forall i, x \in T(q_j, d_i)\}) & \text{if the inequality is } < \\ \max(\{s_j(x) | \forall i, x \in T(q_j, d_i)\}) & \text{if the inequality is } \geq \end{array} \right\}$$

$$L[j,2] = \text{label}(d_j)$$

where $T(q_j, d_i)$ is the trace of the test q_j on the SSTS d_i (see the definition in Section 4). Next, this matrix is sorted according to its first column and all possible threshold values are evaluated in a sequence. α is defined as the threshold with the highest information gain. Algorithm 3 shows the details of these operations:

Algorithm 3: Finding the optimal threshold value α for a new scalar test.

```
input  : $L$: A $n \times 2$ matrix as described in section 6.5.
output: $\alpha$: the optimal threshold

Sort $L$ according to the first column values
$h' \leftarrow +\infty$ ; $i' \leftarrow 0$ ; $w \leftarrow false$
$X \leftarrow \{0\} \times C$ with $C$ the number of classes
$Y \leftarrow$ such that $Y_i$ is the number of SSTS of class $c_i$
for $i \leftarrow 1$ to $n-1$ do
    $X_{L[i,2]} \leftarrow X_{L[i,2]} + 1$
    $Y_{L[i,2]} \leftarrow Y_{L[i,2]} - 1$
    if $L[i+1,1] \neq L[i,1] \wedge (L[i+1,2] \neq L[i,2] \vee w)$ then
        $w \leftarrow false$
        $h \leftarrow entropy(X)i + entropy(Y)(n-i)$
        if $h < h'$ then
            $h' \leftarrow h$ ; $i' \leftarrow i$
    else
        $w \leftarrow true$
$\alpha \leftarrow (L[i',1] + L[i'+1,1])/2$
```

6.6 Finding the Optimal Segment of R

Operations O2 and O4 require specification of a time constraint. In this work, we restrict time constraints to be contiguous segments $[a,b] \in \mathbb{R}$, albeit in general this restriction can be lifted without harm. The data set being finite, the number of meaningful candidate boundaries for a and b is also finite.

Given a GTC A and an operation O2 or O4 to apply, we define $M(d_k) \subset \mathbb{R}$ as follows. For operation O2, given two tests q_i and q_j of A, M is defined as $M(d_k) = \{x_1 - x_2 | \forall x_1 \in T(q_i, d_k), x_2 \in T(q_j, d_k)\}$. For operation O4, given an existing test q_i of A and an event symbol e_j, M is defined as $M(d_k) = \{x_1 - x_2 | \forall x \in T(q_i, d_k), \exists \langle e_j, x_2 \rangle \in d_k\}$. Note that M is computed from the trace T that is itself computed during the GTC evaluation.

By design, (1) If A is not valid on an SSTS d_k, then $M(d_k)$ is empty; and (2) If A is valid on an SSTS d_k, then the GTC resulting from applying the current operation with constraint $[a,b]$ on A is valid on d_k if and only if $\exists x \in M(d_k)$ such that $x \in [a,b]$.

We define $Y = \bigcup_k M(d_k)$, and Y_i to be the i$^{\text{th}}$ smallest element of Y. Finally, we define Z as the set of all candidate boundaries (i.e. $a, b \in Z$) as $Z_i = \{(Y_i + Y_{i+1})/2\}_{i \in [1,|Y|]} \cup$

$\{Y_1\} \cup \{Y_{|Y|}\}$. In case of large data sets, or in case of small data sets with high risk of over-fitting, the set of candidate Z can be randomly sampled down. Such down sampling is in essence equivalent to attribute sampling used e.g. in Random Forest. In practice, this significantly speeds up the search for the optimal time constraint without reducing the model accuracy because of the redundant nature of the decision tree or decision set models. We observed experimentally that limiting Z to 40 elements (i.e. 40^2 interval candidates) does not impact the models' empirical accuracy.

Finding the segment $[a, b]$ that maximizes the information gain is an optimization problem in a finite and countable two dimensional space. The naive and direct solution to this problem requires evaluating a GTC on each SSTS for each unique point in the search space (i.e. for each possible $(a, b) \in Z^2$ with $a < b$). This solution leads to the worst case computational cost of $O(|Z|^2 nE)$ with n being the number of SSTSs and E the computational cost to compute the instances of a GTC on an SSTS. This cost may easily become prohibitively expensive for any realistically complex application. An alternative, more efficient solution is to iterate over M to evaluate application of the GTC. This solution only requires evaluating the initial GTC once, it does not require evaluating the resulting GTC, and it has a computational cost of $O(|Z|^2 n + En)$. It allows us to handle much larger problems than when using the naive approach.

Instead of these two implementations, we propose a third solution with a time complexity of $O(|Z|^2 + nE)$ (instead of $O(|Z|^2 nE)$ of $O(|Z|^2 n + En)$, as above). This new approach relies on the two following properties: (1) If $h \in M(d_k)$, then the GTC resulting from the current operation with the time constraint $[h, h]$ is true on the SSTS d_k; (2) If the GTC with the new constraint $[a, b]$ is true on the SSTS d_k, then all GTCs with a time constraint $[a', b'] \supset [a, b]$ will also be true on the SSTS d_k.

The last solution relies on building a $|Z| \times |Z| \times (C - 1)$ matrix P where C is the number of classes in the classification problem. After being built, each element of $P[x, y, z]$ represents the number of SSTSs in training data which belong to class z and that match the GTC A after it was subjected to the new operation with the time constraint $[Z_x, Z_y]$. Once the matrix P is computed, search for the optimal time constraint can be done in one pass over P by iterating over x and y, then over z in the inner loop. Algorithm 4 shows how to efficiently construct matrix P. Note that in practice, search for the optimal time constraint can be merged with the last "for" loop of the algorithm. Figure 6 illustrates the Algorithm 4 step by step using a small example. Also note that while we use P to optimize information gain, P can be used to optimize any metric that relies on GTC matching counts.

7. Experimental Evaluation

In this section we report and discuss performance of the two proposed algorithms (GTC-DF and GTC-Set) as compared to a wide variety of alternative approaches found in literature. The algorithms are evaluated on a collection of 59 unique data sets described below. All these data sets are publicly available online.

7.1 Synthetic Data (1 set)

The synthetic data set is composed of a relatively simple collection of 200 computer-generated, purely symbolic SSTSs. Each of them contains one instance of each type of

Algorithm 4: Building matrix P.

```
input  : $Z$: The set of candidate boundaries.
         $M$: The "meet" sets.
output: $P$: Matrix $P$.
// a. Initialization
$P \leftarrow$ a $|Z| \times |Z| \times (C-1)$ matrix filled with zeros
for $k = 1$ to $|D|$ do
    $k \leftarrow -1; c \leftarrow$ class of $d_k$
    if $c = C$ then continue
    $m \leftarrow M(d_k)$ // $m_i$ is the i$^{\text{th}}$ smallest element of $m$.
    for $i = 1$ to $|m|$ do
        $j \leftarrow$ such that $Z_j \leq m_i < Z_{j+1}$ // Note: $i \mapsto j$ is monotonically increasing
        $P[j, j, c] \leftarrow P[j, j, c] + 1$
        if $k \neq -1$ then $P[j, k, c] \leftarrow P[i, k, c] - 1$
        $k \leftarrow i$
// b. Vertical upward spread
for $i = 1$ to $|Z|$ do
    $X \leftarrow \{0\} \times (C-1)$
    for $j = i$ to $|Z|$ do
        $X \leftarrow X + P[j, i, \_]$
        $P[j, i, \_] \leftarrow X$
// c. Horizontal left spread
for $i = 1$ to $|Z|$ do
    $X \leftarrow \{0\} \times (C-1)$
    for $j = i$ to $1$ do
        $X \leftarrow X + P[i, j, \_]$
        // Note: Here $X$ contains the class distribution for the candidate GTC
           with time constraints $[Z_j, Z_i]$.
        $P[i, j, \_] \leftarrow X$
```

events from the set A, B and C, respectively at times t_a, t_b and t_c. For each SSTS, t_a is sampled uniformly from $[0, 200]$, and t_b and t_c are sampled uniformly from $[t_a - 15, t_a + 15]$. If $|t_a - t_b| < 10$ and $|t_a - t_c| < 10$ and $|t_b - t_c| < 10$, then the SSTS is labeled as class 1. Else, if $|t_a - t_b| < 10$, then the SSTS is labeled as class 2. If none of these conditions are valid, the SSTS is labeled as class 3. This data set aims to evaluate our algorithm capability of correctly learning temporal constraints from data. The synthetic data set as well as a Python script used to generate it are available at *mathieu.guillame-bert.com/dataset.*

7.2 UCR Time Series Classification Repository (41 UCR Data Sets)

The University of California at Riverside (UCR) benchmark data is a collection of 41 diverse data sets representing time series classification problems of varying complexity. These data sets have the particularity to be *aligned* i.e. given a data set, the i-th observations of all time series reflect the same phenomenon observed at the same moment of time. Because of this alignment, "visual" measures of distance between instances of such data (e.g. Euclidean or

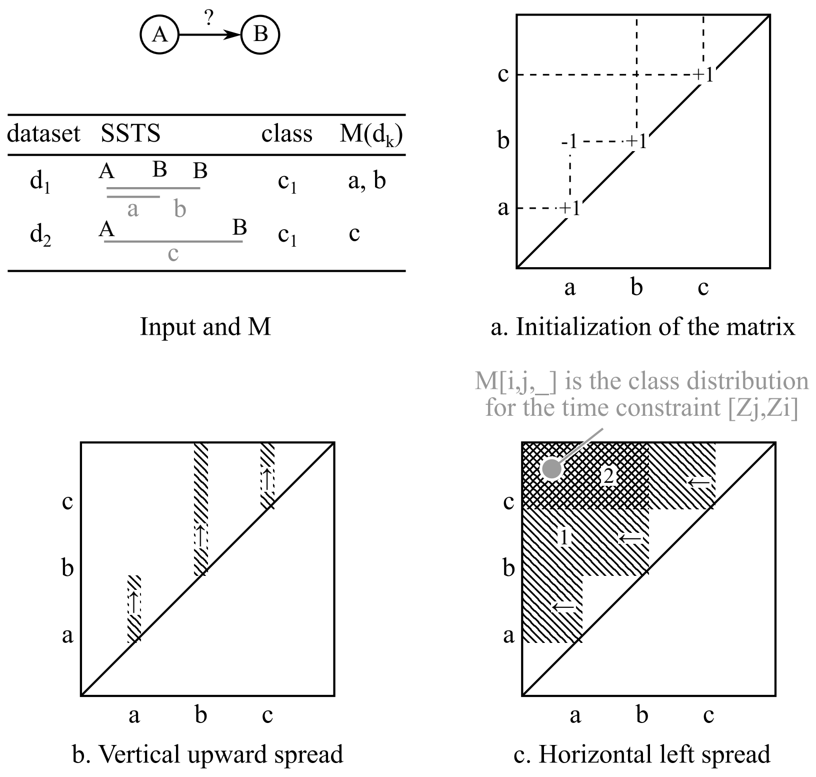
A
?
B
dataset
SSTS
class
M(d_k)
d1
A B B
a b
c1
a, b
d2
A B
c
c1
c
Input and M
c
b
a
+1
-1
+1
+1
a b c
a. Initialization of the matrix
M[i,j,_] is the class distribution for the time constraint [Zj,Zi]
2
1
b. Vertical upward spread
c. Horizontal left spread

Figure 6: Step by step illustration of Algorithm 4 to construct M, matrix P, and the optimal time interval constraint.

Dynamic Time Warping (DTW) restricted to a very small shift coupled with one nearest neighbor) and algorithms designed for "flat" data sets (such as e.g. SVM) can be very competitive. The UCR data sets are organized into two groups: Group 1 (18 sets) and Group 2 (23 sets). The number of classes, number of time series, and their lengths, vary in these data sets respectively from-to $[2, 50]$, $[56, 7164]$ and $[60, 637]$ for Group 1, and $[2, 25]$, $[322, 9236]$ and $[28, 1882]$ for Group 2. It appears that the sets in Group 2 are on average larger than sets of Group 1. These data are available at *http://www.cs.ucr.edu/∼eamonn/time_series_data*.

7.3 16 Rotated UCR Data Sets

The UCR data sets are *aligned*, and it is likely that some classification models applied to them may rely on and benefit from this alignment. These data sets also contain rich local patterns. We propose to modify the UCR data by breaking their alignment in order evaluate the ability of classification algorithms to learn discriminative local patterns. In this way, the modified UCR collection can be used to evaluate algorithms on the significant problem of classifying non-aligned time series and SSTSs. One such scenario involves problems where the starting point of time series observation is arbitrary, which is the case of many practical applications in which we may not have the luxury of observing a modeled process from a

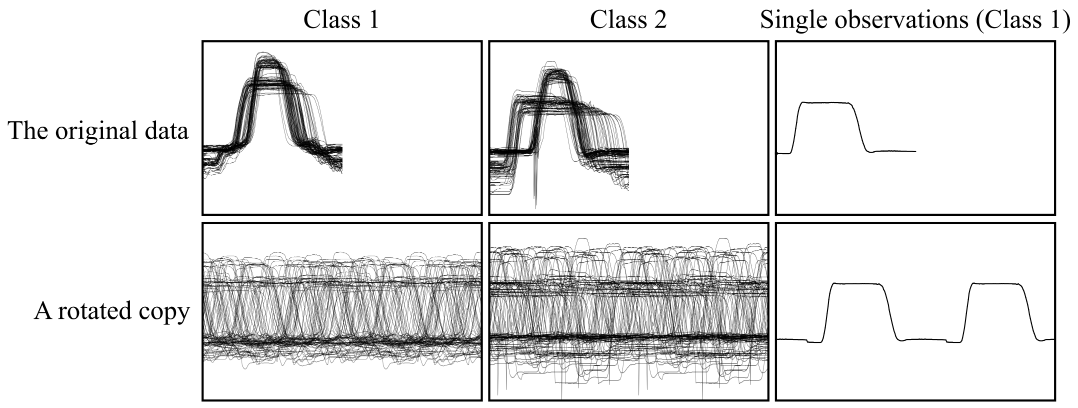

Figure 7: The original and one rotated copy of the UCR Gun Point data set.

well-defined initial setting. We call this modified collection of benchmark data the "Rotated UCR data sets".

The rotation is performed as follows: We break any potentially pre-existing alignment of a data set by randomly and independently shifting each time series in it versus others. Given a time series $X = [x_1, \ldots, x_n]$, the rotated copy is defined as $X' = [x_i, \ldots, x_n, x_1, \ldots, x_n, x_1, \ldots, x_{i-1}]$ with i being a uniformly random integer drawn from the range $[1, n]$ and unique to each time series. In order to avoid disturbing local patterns (if they exist), the rotated series are doubled in length with regard to the originals. To enable comprehensive evaluation, we independently generate 10 rotated copies for each of the originals and use each of these copies independently in experiments. The reported classification performance will be computed by averaging the results obtained from the 10 rotated copies. To avoid excessive computation costs, we chose to rotate all but two UCR Group 1 sets. As an example, Figure 7 shows the original UCR Gun Point data and one of its rotated copies.

7.4 Internal Bleeding Detection Data Set (1 Set)

Undetected internal bleeding during and after surgical procedures is a major medical concern. Early and reliable detection of internal bleeding is therefore considered a significant medical research problem. We assembled the *Bleeding Detection Data Set* from vital signs measured at high frequency (250Hz) using a bed-side hemodynamic monitoring system. The collected measurements include arterial blood pressure, central venous pressure, and airway pressure. The data has been collected from a cohort of 52 healthy pigs subjected to induced slow bleeding. Each animal has been sedated, instrumented, left to rest for half an hour, and then bled at the fixed rate of 20mL/min. From the vital sign records of each pig, we randomly sampled two 30 second long segments of data: One from the resting period before and one approximately 2 minutes into the bleeding. Pre- and post-bleeding segments are respectively labeled as negative and positive. Unlike in the UCR data sets, the SSTSs (vital signs) are not temporally aligned: The starting point of observation is effectively arbitrary. Moreover, the data is multivariate.

For reference, current clinical practice is usually unable to detect internal bleeding earlier than 10 to 15 minutes after the onset of a slow internal bleeding episode. We try to push

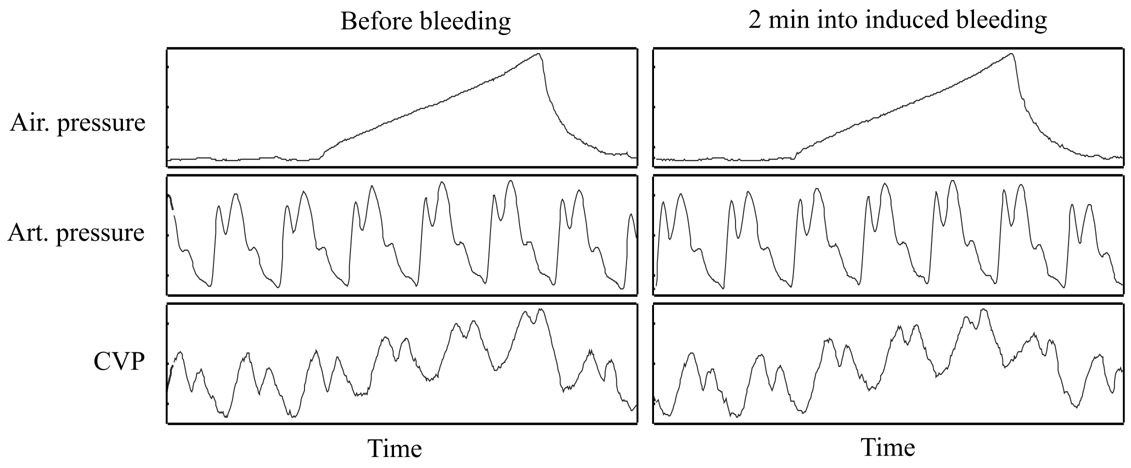

Figure 8: Four second samples of vital sign time series collected from one pig in pre-bleed phase (left) and 2 minutes into the induced bleeding (right). Note that in practice, vital signs of different animals tend to look less similar than vital signs of a same animal before and after bleeding. Air. pressure stands for Airway pressure. Art. pressure stands for arterial blood pressure, and CVP stands for central venous pressure.

that limit by considering SSTSs observed at a 2 minute mark into bleeding, when the data is not yet visually differentiable to expert clinicians. Figure 8 shows small parts of the pre-bleed and 2-minutes-in snapshots of vital signs data observed for one animal. The internal bleeding detection data set is available at *mathieu.guillame-bert.com* [Guillame-Bert].

7.5 Experimental Setup

Purposive featurization of time sequence data can sometimes significantly impact performance of the resulting models. In order to avoid obfuscating the relative performance of various algorithms being compared in this paper, we decided to not invest time and effort to produce advanced and potentially informative algorithm-specific featurizations of raw data. Instead, we relied on two basic statistics (moving averages and moving standard deviations), and we marked easily detectable peaks manifesting in the scalar data using a simple threshold criterion on the signal's second order derivative.

All considered algorithms have been implemented (or re-implemented) in C++ to ensure fairness of comparison. The computation times reported include training and evaluation over the complete 10-fold cross-validation cycles. This allows fair comparisons of lazy (e.g. 10NN) and non-lazy (e.g. our methods) algorithms. Experiments have been performed on a 3.4GHz i7 8-core processor with 16GB of main memory. Multiple algorithms were slow when applied on the UCR data set *StarLightCurves* (StarLC). Algorithms taking more than one day of computation for the 10-fold cross-validation were stopped and the expected total computation cost was estimated from the completed iterations. For this reason, results on *StarLightCurves* data are not used in computation of the global rankings.

7.6 Results

We compare our two algorithms against 13 related and relevant alternative classification algorithms for time series. The reference list includes: *ED+NN*: Euclidean Distance (i.e. L_2 distance) with Single Nearest Neighbor (Ding et al., 2008), *ED+kNN*: Euclidean Distance with k Nearest Neighbors (k is specified by the user), *ED+CVkNN*: Euclidean Distance with k Nearest Neighbors (k is determined through an internal loop 10-fold cross-validation executed on each training fold of the main 10-fold cross-validation loop), *DTW+NN*: Dynamic Time Warping (Berndt and Clifford, 1994) with Single Nearest Neighbor, *DTWC+NN*: Dynamic Time Warping with Constrained Warping Window (Berndt and Clifford, 1994) with Single Nearest Neighbor, *EDR+NN*: Edit Distance on Real Sequence (Chen and Ng, 2004) with Single Nearest Neighbor, *ERP+NN*: Edit Distance with Real Penalty (Chen et al., 2005) with Single Nearest Neighbor, *LCSS+NN*: Longest Common Subsequence (Vlachos et al., 2002) with Single Nearest Neighbor, *LCSSC+NN*: Longest Common Subsequence with Constrained Warping Window (Vlachos et al., 2002) with Single Nearest Neighbor, *L-1+NN*: L_1 distance with Single Nearest Neighbor, *L-inf+NN*: L_∞ distance with Single Nearest Neighbor, *RF*: Random Decision Forest (Breiman, 2001), *SVM*: Support Vector Machine Meyer et al., 2003, *Default*: Always return the most frequent class.

Algorithm parameters have not been tuned and were assigned to their meaningful default settings (except for k in *ED+kNNCV*), as follows. *RF*: maxNumTrees(30), minNumObservations(5), maxDepth(10). *LCSS+NN*: e(0.05 standard deviation). *EDR+NN*: e(0.25 standard deviation). *LCSSC+NN*: The maximum window is set to 25% of the data set length. It is worth noting that one could argue that the maximum window setting (c) of 25% is too high to operate DTWC and LCSSC on the UCR data sets, but we have chosen that for the three following reasons. Firstly, we have not tuned any algorithm parameters for specific data sets except for k in *ED+kNNCV*. Secondly, we have evaluated Euclidean Distance method being equivalent to DTWC with c=0%, and DTW being equivalent to DTWC with c=100%. Thirdly, c is a constraint parameter that only and strictly expands search space of the closest element when increased. We have experimented with alternative settings of this parameter and we have indeed obtained slight variations of empirical accuracy of DTWC, but these variations have not materially changed performance rankings reported below. We therefore chose to evaluate DTWC+NN (and other constrained dynamic programming distances) with c=25% for consistency. It is significant to remark that we evaluated the original implementation of DTW (Berndt and Clifford, 1994). Several pruning criteria have been studied to reduce the computation time without impacting the classification performances, including the work of Keogh and Ratanamahatana (2005). *DTWC+NN*: The maximum window is set to 25% of the data set length. *ED+CVkNN*: k is searched between 1 and 10. It is likely that optimizing parameters of each algorithm using internal cross-validation might improve their results, but it would significantly increase the computation time.

All reported results have been computed using the same 10-fold partitioning of data. In the case of the rotated UCR data sets, the 10-fold cross-validation is repeated for each of the 10 rotations of each rotated data set (e.g. each reported error rate is computed from 100 train and test experiments). In Bleeding Detection Data Set, we ensure that the complete record for each animal is either entirely used for training or for testing in each cross-validation iteration.

Reported evaluation figures for the UCR data sets are not directly comparable with figures reported by Ding et al. (2008) or the figures available on the UCR Time Series web page: In Ding et al. (2008), evaluation results are computed with a "reversed cross-validation" where each of the n folds is successively used for training while the remaining $n-1$ folds are used for testing. On the UCR Time Series web page, evaluation is performed with a train and test protocol.

Tables 1 and 3 respectively compile the observed classification errors of all algorithms on the UCR data sets and rotated UCR data sets. The average rank and median rank are also reported for each algorithm. Table 2 shows the cumulative computation times of training and testing cycles for each algorithm. Table 4 shows the accuracy, classification error, AUC scores and computation times of each algorithm when applied to the Bleeding Detection Data Set. Figure 9 shows the ROC of the GTC-DF and Random Forest models obtained for this data set.

First, both our algorithms show a 100% accuracy on the synthetic data. This simple experiment validates their ability to identify explicit temporal sequence patterns when they exist.

The experiments on the UCR data, rotated UCR data, and Bleeding Detection Data Set (Tables 1, 3 and 4), show consistently high performance of our algorithms in comparison to state-of-the-art alternatives. On the original UCR data, and when considering 13 other methods, GTC-DF and GTC-Set have the highest average and median ranks of accuracy (respectively a median rank of 2 and 2.5 for Group 1, and 2.5 and 2.5 for Group 2). The next best methods are ERP+NN (med. rank of 4.8) and DTW+NN (med. rank of 6) for Group 1, and SVM (med.rank of 4.5) and ERP+NN (med. rank of 5) for Group 2. It is worth noting that since the original UCR data sets are internally aligned, methods that rely on basic distance metrics (e.g. Euclidean Distance or DTWC with very strong constraints e.g. c=0.5%) tend to perform relatively well and are also cheap to compute.

The Wilcoxon signed-rank test (Demšar, 2006) was applied to evaluate the significance of differences of performance between each algorithms. The resulting p-values are reported in Table 5. GTC-DF performs significantly better than all the other evaluated methods (including GTC-Set). Additionally, GTC-Set, while performing significantly worse than GTC-DF, performs significantly better than all the other evaluated methods.

Table 1: Empirical classification error rates observed for the algorithms under consideration on the UCR data sets from Groups 1 and 2. The first column contains the acronym names of the algorithms (our methods are labeled GTC-DF and GTC-Set), and the next two columns show average rank and median rank of each algorithm based on their accuracy performance measured on the individual data sets. The algorithms are sorted according to their average rank, and the two proposed methods top the sorted list.

(a) Error rates for the UCR Group 1 data sets.

Algo.	avg.rank	med.rank	50words	Adiac	Beef	CBF	Coffee	ECG200	FaceAll	Face4	GunPoint	Lighting2	Lighting7	OSULeaf	Trace	2Patterns	Fish	Synthetic	Wafer	Yoga
GTC DF	**3.5**	**2**	.225	**.237**	.300	.005	**.036**	.115	.045	.018	.015	.223	**.196**	.242	**.000**	.001	**.066**	**.007**	**.000**	.045
GTC Set	3.7	2.5	.235	.256	**.250**	.004	**.036**	.120	.045	.018	**.010**	.223	.203	.265	**.000**	.001	.074	.012	.001	.045
ERP+NN	4.8	5.5	.254	.344	.550	**.000**	.107	.125	.010	.018	.015	**.107**	.315	.240	.090	**.000**	.143	.023	.002	.037
DTW+NN	5.9	6	.261	.359	.550	**.000**	.107	.175	.012	.027	.060	.132	.294	.269	.005	**.000**	.177	.018	.003	.055
DTWC+NN	5.9	6	.250	.359	.550	**.000**	.089	.175	.012	.027	.060	.132	.301	.269	.005	**.000**	.177	.018	.003	.062
EDR+NN	6.7	5	**.171**	.830	.567	.009	**.036**	.105	**.008**	**.009**	.055	.182	.308	**.143**	.030	**.000**	.226	.112	.002	.073
SVM	7.1	6.5	.277	.344	.667	.002	.071	.115	.023	.062	.015	.248	.350	.301	.130	.013	.094	.018	.001	.042
RF	7.8	8.5	.349	.297	.517	.002	.268	.120	.051	**.009**	.025	.190	.238	.367	.080	.012	.189	.023	.004	.066
ED+NN	8.1	9	.322	.329	.517	.009	.125	.105	.038	.071	.050	.231	.343	.342	.130	.013	.174	.078	.001	.056
L1+NN	8.3	8	.282	.350	.550	.015	.143	**.065**	.031	.027	.050	.190	.322	.328	.135	.003	.191	.100	.002	.056
LCSSC+NN	9.5	11	.360	.362	.550	.012	.161	.210	.279	.152	.035	.223	.441	.176	.060	.002	.091	.270	.004	**.027**
LCSS+NN	9.6	11	.360	.362	.550	.012	.161	.215	.283	.152	.035	.223	.441	.179	.060	.001	.091	.262	.004	**.027**
ED+5NN	11.3	11	.345	.387	.550	.009	.304	.110	.080	.125	.095	.281	.378	.391	.315	.020	.180	.092	.003	.078
Linf+NN	12.4	14	.429	.306	.483	.181	.071	.135	.148	.268	.095	.372	.580	.389	.150	.693	.171	.137	.007	.083
ED+CVkNN	12.6	14	.402	.435	.567	.008	.286	.095	.111	.152	.120	.355	.427	.457	.445	.032	.211	.113	.004	.097
ED+10NN	12.6	14	.402	.435	.567	.008	.286	.095	.111	.152	.120	.355	.427	.457	.445	.032	.211	.113	.004	.097
default	17.0	17	0.88	0.986	0.983	0.712	0.625	0.335	0.855	0.696	0.62	0.397	0.734	0.781	0.85	0.739	0.937	0.885	0.106	0.464

(b) Error rates for the UCR Group 2 data sets.

Algo.	avg.rank	med.rank	ChlorineC	ECGtorso	CricketX	CricketY	CricketZ	DiatSRed	ECG5D	FacesUCR	Haptics	InlineS	ItPwrDmd	MALLAT	MedImgs	MoteStrain	SonyRbtS	SonyRbtS2	Symbols	2LeadECG	WordsSyn	uWvGLibX	uWvGLibY	uWvGLibZ	StarLC*
GTC DF	**4.3**	**2.5**	.194	.004	.171	**.167**	**.162**	.006	**.000**	.040	.475	.348	.031	**.000**	**.155**	.039	.011	.035	.021	.003	.210	.158	**.215**	**.206**	**.022**
GTC Set	4.5	**2.5**	.236	.001	**.169**	.171	.173	.006	.001	.044	.473	**.335**	.033	**.000**	.162	.039	.016	.036	.020	.003	.224	**.156**	.221	.209	.025
SVM	4.6	4.5	.045	**.000**	.291	.279	.272	.003	**.000**	.021	**.467**	.423	.034	.017	.191	.057	**.006**	**.006**	.031	**.002**	.267	.184	.255	.243	.029
ERP+NN	5.7	5	.008	.002	.212	.177	.208	.003	.005	**.011**	.540	.395	.045	.006	.199	.031	.018	.017	.023	**.002**	.228	.221	.298	.274	2.000
DTW+NN	7.0	8	.008	.001	.321	.309	.328	**.000**	.003	.032	.605	.469	.037	.006	.215	.031	.021	.012	.034	.006	.256	.228	.283	.296	2.000
DTWC+NN	7.0	8	.008	.001	.321	.309	.328	**.000**	.003	.032	.605	.469	.037	.006	.215	.031	.021	.012	.034	.006	.256	.228	.283	.296	2.000
L1+NN	7.0	8	.008	.001	.321	.309	.328	**.000**	.003	.032	.605	.469	.037	.006	.215	.031	.021	.012	.034	.006	.256	.228	.283	.296	.111
LCSS+NN	7.3	5.5	.077	.003	.276	.219	.264	.019	.005	.028	.533	.415	.059	.026	.225	**.023**	.095	.105	**.014**	**.002**	**.177**	.208	.286	.263	2.000
LCSSC+NN	7.3	6	.077	.003	.277	.219	.263	.019	.005	.029	.533	.415	.059	.026	.225	**.023**	.095	.105	**.014**	**.002**	**.177**	.208	.286	.262	2.000
RF	7.5	7	.214	.008	.262	.251	.282	.016	.015	.053	.527	.458	**.026**	.003	.193	.036	.013	.034	.032	.019	.319	.197	.247	.233	.035
ED+NN	8.3	9	**.003**	.001	.341	.346	.332	**.000**	.005	.040	.583	.477	.034	.015	.230	.079	.014	.015	.035	.004	.284	.229	.274	.291	.111
ED+5NN	10.5	12	.078	.004	.421	.371	.415	.016	.014	.078	.577	.546	.027	.020	.240	.079	.018	.031	.041	.004	.330	.236	.274	.287	.117
ED+CVkNN	11.6	13	.171	.006	.503	.406	.486	**.000**	.029	.109	.583	.618	.034	.021	.264	.071	.023	.041	.049	.005	.381	.247	.275	.297	.137
ED+10NN	12.1	13	.171	.006	.503	.406	.486	.019	.029	.109	.583	.618	.034	.021	.264	.071	.023	.041	.049	.005	.381	.247	.275	.297	.137
EDR+NN	12.1	16	.572	.001	.317	.285	.286	.677	.002	.027	.680	.782	.192	.356	.350	.065	.027	.023	.186	.507	.265	.263	.394	.378	2.000
Linf+NN	12.3	15	.019	.014	.563	.529	.578	**.000**	.002	.148	.613	.514	.036	.035	.274	.153	.024	.034	.047	**.002**	.391	.259	.317	.318	.120
default	17.0	17	.464	.789	.967	.960	.964	.764	.529	.855	.819	.834	.526	.910	.479	.461	.438	.384	.847	.539	.779	.897	.897	.897	.423

Table 2: Computing times of training and testing on the UCR data sets from Groups 1 and 2. Sorting of algorithms is the same as in Table 1b. Note that our algorithms very often remain competitive in terms of computational costs when compared to the most accurate alternatives. The ordering of the algorithms in this table is the same as in Table 1b. The bottom part of each table summarizes basic statistics of the data sets. Color is used to indicate value of each cell and it is normalized separately for each column.

(a) Computing times for the UCR Group 1 data sets

Algo.	avg.rank	med.rank	50words	Adiac	Beef	CBF	Coffee	ECG200	FaceAll	Face4	GunPoint	Lighting2	Lighting7	OSULeaf	Trace	2Patterns	Fish	Synthetic	Wafer	Yoga
GTC DF	3.5	2	51mn 39s	12mn 1.6s	12s	1mn 35s	3.6s	19s	**1h 9mn 52s**	24s	14s	30s	**2mn 34s**	6mn 20s	18s	2h 21mn	2mn 46s	1mn 46s	10mn 57s	27mn 48s
GTC Set	3.7	2.5	**1h 24mn**	**16mn 2.3s**	12s	2mn 2.7s	4.3s	**26s**	38mn 15s	36s	18s	41s	2mn 3s	12mn 41s	23s	30mn 28s	4mn 5.1s	**3mn 11s**	12mn 0.53s	37mn 3s
ERP+NN	4.8	5.5	24mn 27s	7mn 41s	28s	6mn 56s	**9.5s**	8.7s	35mn 5.9s	37s	21s	2mn 35s	51s	15mn 12s	1mn 13s	**2h 45mn**	11mn 19s	30s	8h 35mn	14h 55mn
DTW+NN	5.9	6	21mn 0.86s	6mn 34s	**30s**	7mn 1.9s	8.2s	11s	29mn 55s	**51s**	**28s**	**4mn 18s**	44s	**20mn 0.7s**	1mn 9.8s	2h 21mn	**16mn 19s**	38s	**9h 14mn**	**15h 8mn**
DTWC+NN	5.9	6	12mn 1.7s	3mn 47s	15s	3mn 8.4s	3.7s	3.4s	15mn 53s	15s	8.4s	1mn 7.4s	25s	6mn 35s	29s	1h 20mn	4mn 51s	12s	3h 46mn	1h 3mn
EDR+NN	6.7	5	21mn 47s	10mn 3.4s	21s	**7mn 7.8s**	6s	8s	30mn 37s	34s	20s	2mn 22s	45s	13mn 58s	1mn 11s	2h 25mn	10mn 52s	27s	7h 8mn	14h 49mn
SVM	7.1	6.5	26s	11s	2.2s	13s	3s	3.6s	27s	5.4s	3.4s	11s	3.4s	23s	7.3s	1mn 13s	18s	5.4s	1mn 17s	2mn 3.5s
RF	7.8	8.5	1mn 20s	44s	4s	12s	2s	3.6s	1mn 43s	1.2s	0.9s	13s	8.1s	53s	9.1s	5mn 2.1s	38s	11s	7mn 28s	9mn 55s
ED+NN	8.1	9	13s	5.3s	0.17s	6.6s	0.11s	0.52s	30s	0.62s	0.64s	1.3s	0.5s	6.5s	1.2s	2mn 25s	4.6s	1.2s	7mn 36s	5mn 35s
L1+NN	8.3	8	14s	5.6s	0.17s	6.6s	0.21s	0.53s	31s	0.39s	0.79s	1.1s	0.51s	7.8s	0.82s	2mn 31s	5.8s	1.5s	7mn 53s	5mn 49s
LCSSC+NN	9.5	11	14mn 14s	3mn 20s	12s	2mn 15s	3s	2.6s	15mn 19s	11s	6.1s	52s	23s	5mn 9.1s	21s	1h 4mn	3mn 36s	9.1s	2h 19mn	5h 30s
LCSS+NN	9.6	11	15mn 37s	5mn 17s	24s	5mn 8s	6.4s	8.3s	31mn 38s	42s	19s	3mn 23s	47s	19mn 2.1s	**1mn 16s**	1h 44mn	11mn 2.1s	21s	6h 4mn	12h 34mn
ED+5NN	11.3	11	3.1s	1.3s	0.11s	1.3s	0.075s	0.13s	6.3s	0.18s	0.15s	0.35s	0.23s	1.4s	0.29s	28s	1.1s	0.32s	1mn 6.5s	55s
Linf+NN	12.4	14	13s	5.5s	0.18s	5.9s	0.19s	0.49s	30s	0.71s	0.43s	0.93s	0.51s	7s	1.4s	2mn 27s	4.9s	1.4s	7mn 45s	5mn 55s
ED+CVkNN	12.6	14	4mn 6.1s	1mn 42s	3s	1mn 34s	2.1s	3.4s	9mn 59s	6.4s	6.2s	14s	9.2s	1mn 39s	14s	47mn 11s	1mn 9.4s	17s	1h 48mn	1h 29mn
ED+10NN	12.6	14	2.6s	1.1s	0.06s	1.1s	0.041s	0.067s	5.6s	0.12s	0.1s	0.22s	0.15s	1.2s	0.21s	28s	0.82s	0.24s	1mn 4.1s	53s
default	**17.0**	**17**	1s	0.38s	0.071s	0.44s	0.043s	0.063s	1.1s	0.11s	0.076s	0.18s	0.14s	0.45s	0.14s	2.1s	0.35s	0.14s	3.1s	3.1s
#classes			50	37	5	3	2	2	14	4	2	2	7	6	4	4	7	6	2	2
length			270	176	470	128	286	96	131	350	150	637	319	427	275	128	463	60	152	426
#ssts			905	781	60	930	56	200	2250	112	200	121	143	442	200	5000	350	600	7164	3300
avg.err.			.341	.410	.545	.058	.171	.142	.126	.117	.087	.239	.370	.329	.172	.092	.200	.134	.009	.083
std.err.			.156	.196	.150	.174	.148	.064	.206	.167	.142	.087	.135	.149	.225	.235	.197	.209	.025	.100

(b) Computing times for the UCR Group 2 data sets

Algo.	avg.rank	med.rank	ChlorineC	ECGtorso	CricketX	CricketY	CricketZ	DiatSRed	ECG5D	FacesUCR	Haptics	InlineS	ItPwrDmd	MALLAT	MedImgs	MoteStrain	SonyRbtS	SonyRbtS2	Symbols	2LeadECG	WordsSyn	uWvGLibX	uWvGLibY	uWvGLibZ	StarLC*
GTC DF	4.3	2.5	47mn 58s	7mn 58s	22mn 30s	19mn 41s	22mn 29s	21s	1mn 23s	30mn 15s	10mn 50s	20mn 3.1s	49s	8mn 16s	11mn 38s	3mn 59s	1mn 4.3s	2mn 42s	4mn 23s	1mn 0.84s	38mn 59s	1h 25mn	1h 34mn	1h 29mn	2h 28mn
GTC Set	4.5	2.5	56mn 6.7s	8mn 20s	**34mn 46s**	**28mn 58s**	**34mn 49s**	23s	**1mn 35s**	**37mn 21s**	14mn 36s	24mn 22s	**56s**	9mn 35s	**13mn 15s**	**4mn 36s**	**1mn 15s**	**3mn 48s**	7mn 35s	1mn 6.5s	**47mn 57s**	1h 58mn	1h 56mn	1h 55mn	3h 13mn
SVM	4.6	4.5	57s	1mn 32s	13s	13s	13s	3.7s	4.2s	19s	24s	1mn 0.85s	1.3s	1mn 25s	6.1s	4.5s	1.7s	2.6s	15s	3.5s	14s	1mn 21s	1mn 28s	1mn 27s	7mn 8s
ERP+NN	5.7	5	48mn 39s	11h 30mn	5mn 18s	5mn 17s	5mn 17s	1mn 17s	1mn 22s	8mn 11s	31mn 41s	3h 12mn	3.9s	12h 37mn	1mn 12s	1mn 4.5s	11s	23s	17mn 47s	51s	5mn 48s	**3h 12mn**	3h 12mn	**3h 12mn**	7day 18h
DTW+NN	7.0	8	1mn 29s	2h 36mn	9.1s	8.6s	8.7s	3.5s	3.1s	17s	6mn 52s	42mn 8s	0.53s	2h 44mn	3.2s	3.3s	0.73s	1.5s	3mn 58s	2.7s	11s	4mn 47s	4mn 49s	5mn 11s	1day 17h
DTWC+NN	7.0	8	1mn 33s	2h 34mn	9s	8.9s	8.8s	2.7s	3.1s	18s	6mn 58s	43mn 24s	0.6s	2h 45mn	3.2s	3.3s	0.72s	1.6s	3mn 59s	2.7s	9.8s	4mn 55s	4mn 49s	4mn 52s	1day 17h
L1+NN	7.0	8	26s	48s	2.5s	2.5s	2.5s	0.64s	1.1s	5.8s	4.2s	13s	0.28s	1mn 20s	1.1s	1.2s	0.36s	0.72s	5.4s	0.97s	2.9s	1mn 12s	1mn 11s	1mn 11s	18mn 39s
LCSS+NN	7.3	5.5	31mn 4.9s	7h 48mn	3mn 21s	3mn 18s	3mn 22s	24s	36s	4mn 52s	25mn 11s	2h 15mn	2.2s	8h 7mn	44s	40s	7.1s	14s	11mn 52s	25s	3mn 6.2s	1h 57mn	1h 58mn	1h 59mn	5day 16h
LCSSC+NN	7.3	6	15mn 33s	4h 47mn	1mn 42s	1mn 41s	1mn 41s	14s	21s	2mn 31s	13mn 32s	1h 20mn	1.4s	4h 57mn	21s	20s	3.6s	7.5s	7mn 0.73s	14s	1mn 42s	1h 7.8s	1h 43s	1h 37s	3day 4h
RF	7.5	7	3mn 25s	6mn 46s	51s	50s	51s	0.61s	16s	1mn 12s	1mn 38s	4mn 56s	4.3s	4mn 6.3s	25s	18s	2.4s	11s	60s	16s	54s	6mn 59s	7mn 17s	7mn 4.7s	1h 1mn
ED+NN	8.3	9	27s	48s	2.7s	2.6s	2.6s	0.77s	1.3s	6.3s	4.4s	13s	0.3s	1mn 20s	1.2s	1.2s	0.39s	0.81s	5.6s	1s	2.6s	1mn 10s	1mn 11s	1mn 8.9s	18mn 43s
ED+5NN	10.5	12	29s	49s	2.7s	2.6s	2.7s	0.73s	1.3s	6.3s	4.3s	13s	0.31s	1mn 21s	1.2s	1.2s	0.43s	0.74s	5.6s	1s	2.9s	1mn 11s	1mn 11s	1mn 12s	18mn 50s
ED+CVkNN	11.6	13	43mn 39s	1h 13mn	3mn 20s	3mn 20s	3mn 21s	43s	1mn 30s	8mn 58s	5mn 27s	18mn 13s	18s	2h 6mn	1mn 27s	1mn 29s	21s	47s	7mn 56s	**1mn 13s**	4mn 1.1s	1h 55mn	1h 56mn	1h 56mn	1day 7h
ED+10NN	12.1	13	28s	48s	2.2s	2.2s	2.2s	0.51s	1s	5.7s	3.6s	12s	0.24s	1mn 17s	1s	1s	0.29s	0.56s	5.5s	1s	2.8s	1mn 11s	1mn 11s	1mn 11s	18mn 36s
EDR+NN	12.1	16	**57mn 7.8s**	**11h 59mn**	5mn 17s	5mn 23s	5mn 27s	**2mn 32s**	1mn 32s	7mn 41s	**32mn 41s**	**3h 27mn**	5.1s	**14h 26mn**	1mn 31s	1mn 0.88s	11s	21s	**19mn 41s**	1mn 5.7s	5mn 39s	3h 4mn	**3h 14mn**	3h 11mn	**8day 20h**
Linf+NN	12.3	15	31s	48s	2.5s	2.6s	2.5s	0.67s	1.4s	6.7s	4.1s	13s	0.25s	1mn 16s	1.1s	1.1s	0.28s	0.52s	5.5s	1s	3s	1mn 12s	1mn 13s	1mn 12s	18mn 27s
default	**17.0**	**17**	0.83s	1.6s	0.19s	0.2s	0.19s	0.075s	0.11s	0.36s	0.32s	0.76s	0.048s	1.7s	0.12s	0.12s	0.058s	0.088s	0.28s	0.098s	0.19s	1.1s	1.1s	1.1s	6.5s
#classes			3	4	12	12	12	4	2	14	5	7	2	8	10	2	2	2	6	2	25	8	8	8	3
length			166	1639	300	300	300	345	136	131	1092	1882	24	1024	99	84	70	65	398	82	270	315	315	315	1024
#ssts			4307	1420	780	780	780	322	884	2250	463	650	1096	2400	1141	1272	621	980	1020	1162	905	4478	4478	4478	9236
avg.err.			.138	.050	.367	.336	.362	.091	.038	.099	.577	.505	.075	.087	.241	.078	.052	.055	.089	.066	.305	.259	.316	.314	.780
std.err.			.165	.190	.191	.187	.191	.238	.127	.198	.084	.139	.122	.228	.077	.104	.103	.089	.199	.172	.139	.168	.155	.156	.933

Table 3: Classification error rates observed on the rotated UCR data sets. "O." stands for the original and "R." for the rotated data. The average and median ranks only reflect the rotated results. Algorithms are sorted according to their average rank on the rotated data sets. Note that GTC-DF and GTC-Set are consistently the highest on average ranking algorithms, while the runner-ups change when compared to the non-rotated data results.

Algo.	avg.rank	med.rank	50words		Adiac		Beef		CBF		Coffee		ECG200		FaceAll		Face4		GunPoint		Lighting2		Lighting7		OSULeaf		Trace		2Patterns		Fish		Synthetic	
			O.	R.	O.	R.	O.	O.	R.	O.	R.	O.	O.	R.	O.	R.	O.	R.	O.	R.	O.	R.	O.	R.	O.	R.	O.	R.	O.	R.	O.	R.	O.	R.
GTC DF	**2.9**	**2**	.220	**.359**	**.243**	**.308**	.300	.667	.004	.008	**.036**	.320	.105	**.166**	.044	.060	.018	.188	**.015**	**.043**	.190	.217	**.203**	.290	.242	.232	**.000**	.006	.001	.081	.077	**.170**	**.008**	.171
GTC Set	3.6	2.5	.239	.379	.259	.317	**.267**	.658	.004	.011	**.036**	.338	.115	.168	.048	.066	.018	.188	**.015**	.050	.231	.240	**.203**	**.288**	.247	.245	**.000**	**.004**	.001	**.080**	**.063**	.184	**.008**	**.169**
ERP+NN	4.4	5	.254	.459	.344	.651	.550	.623	**.000**	**.000**	.107	.371	.125	.177	.010	**.027**	.018	.060	**.015**	.112	**.107**	**.172**	.315	.349	.240	.298	.090	.222	**.000**	.112	.143	.320	.023	.205
DTWC+NN	6.4	6.5	.250	.630	.359	.859	.550	.617	**.000**	.042	.089	.445	.175	.256	.012	.329	.027	.525	.060	.254	.132	.312	.301	.495	.269	.465	.005	.349	**.000**	.109	.177	.633	.018	.337
DTW+NN	6.5	7	.261	.630	.359	.859	.550	.617	**.000**	.042	.107	.445	.175	.256	.012	.329	.027	.525	.060	.254	.132	.312	.294	.495	.269	.465	.005	.349	**.000**	.109	.177	.633	.018	.337
LCSS+NN	6.8	5.5	.360	.360	.362	.865	.550	.757	.012	.001	.161	.293	.215	.182	.283	.060	.152	**.017**	.035	.062	.223	.210	.441	.374	.179	**.146**	.060	.095	.001	.107	.091	.251	.262	.253
LCSSC+NN	6.8	5.5	.360	.360	.362	.865	.550	.757	.012	.001	.161	.293	.210	.182	.279	.060	.152	**.017**	.035	.062	.223	.210	.441	.374	.176	**.146**	.060	.095	.002	.107	.091	.251	.270	.253
EDR+NN	7.3	6	**.171**	.546	.830	.977	.567	.800	.009	.012	**.036**	**.287**	.105	.227	**.008**	.105	**.009**	.156	.055	.397	.182	.317	.308	.522	**.143**	.348	.030	.549	**.000**	.104	.226	.864	.112	.235
L1+NN	8.0	8	.282	.630	.350	.859	.550	.617	.015	.040	.143	.466	**.065**	.257	.031	.329	.027	.519	.050	.267	.190	.320	.322	.495	.328	.462	.135	.340	.003	.109	.191	.631	.100	.339
SVM	8.9	10	.277	.658	.344	.882	.667	.648	.002	.031	.071	.559	.115	.263	.023	.435	.062	.627	**.015**	.218	.248	.413	.350	.682	.301	.470	.130	.430	.013	.137	.094	.591	.018	.253
RF	9.0	10	.349	.751	.297	.941	.517	**.587**	.002	.048	.268	.500	.120	.311	.051	.578	**.009**	.609	.025	.214	.190	.347	.238	.531	.367	.532	.080	.334	.012	.159	.189	.689	.023	.290
ED+NN	9.2	10	.322	.665	.329	.848	.517	.615	.009	.059	.125	.484	.105	.262	.038	.413	.071	.588	.050	.333	.231	.445	.343	.661	.342	.474	.130	.495	.013	.120	.174	.611	.078	.360
ED+5NN	11.5	12	.345	.721	.387	.924	.550	.607	.009	.045	.304	.507	.110	.274	.080	.600	.125	.686	.095	.384	.281	.440	.378	.720	.391	.518	.315	.659	.020	.116	.180	.754	.092	.359
Linf+NN	12.4	13.5	.429	.767	.306	.812	.483	.630	.181	.412	.071	.500	.135	.279	.148	.625	.268	.724	.095	.404	.372	.463	.580	.780	.389	.517	.150	.636	.693	.759	.171	.585	.137	.479
ED+10NN	13.4	14	.402	.750	.435	.947	.567	.612	.008	.076	.286	.521	.095	.282	.111	.678	.152	.738	.120	.449	.355	.513	.427	.760	.457	.563	.445	.723	.032	.135	.211	.805	.113	.405
default	16.5	17	.880	.880	.986	.986	.983	.983	.712	.712	.625	.625	.335	.335	.855	.855	.696	.696	.620	.620	.397	.397	.734	.734	.781	.781	.850	.850	.739	.739	.937	.937	.885	.885

Algorithm	Error rate	Accuracy	Duration	AUC
GTC DF	0.087	**0.913**	18mn	**0.975**
GTC Set	0.125	0.875	2h	0.958
ERP+NN	0.404	0.596	**36h**	0.524
LCSS+NN	0.423	0.577	32h	0.519
LCSSC+NN	0.423	0.577	9h	0.519
EDR+NN	0.462	0.538	**36h**	0.51
DTW+NN	0.471	0.529	1h	0.507
DTWC+NN	0.471	0.529	1h	0.507
L1+NN	0.471	0.529	24s	0.507
RF	0.471	0.529	7mn	0.507
ED+10NN	0.5	0.5	2.7s	0.500
SVM	0.5	0.5	3mn	0.488
default	0.5	0.5	0.67s	0.500
Avg. Vit	0.51	0.49	3.9s	0.492
ED+NN	0.529	0.471	26s	0.493
Linf+NN	**0.577**	0.423	25s	0.481

Table 4: Classification error, accuracy, computation time (of the complete 10-fold cross-validation cycle), and AUC obtained on the bleeding detection data set. GTC methods are by far the top performers on this data.

The rotated UCR data sets are harder to classify than the original, aligned UCR data sets. In most cases, the error rates on the rotated data sets are higher for the same algorithm than the rates observed on the non-rotated counterparts (see Table 3). The experiment shows that GTC-DF and GTC-Set are substantially less impacted by this randomization than any other of the evaluated methods, and that GTC-DF and GTC-Set remain the top performers in terms of the average and median ranks (respectively an average and median rank of 2.9 and 2 for GTC-DF, and 3.6 and 2.5 for GTC-Set (Table 3). As expected, GTC-DF and GTC-Set yield similar error rates, and therefore their ranking impact each other. Removing one of these two algorithms from the ranking would further increase the ranking difference between the remaining proposed algorithm and the other state of the art methods under consideration.

Finally, on the Bleeding Detection Data Set, GTC-DF shows an Area Under the Receiver Operating Characteristic Curve (AUC) score of 96.2% and the accuracy at the default sensitivity set point (50%) of 91.3%, while all other evaluated methods show performance very close to random based on their empirical AUC scores (Table 4). This last result is encouraging as it may allow developing effective cardio-respiratory monitors tailored to detect specific hard-to-discern conditions.

In addition to overall highly competitive performance, learning of GTC-DF and GTC-Set models is reasonably fast, even though these algorithms are not uniformly faster than all of the evaluated alternatives. The 10-fold cross-validation on the Yoga data set (the largest of the considered sets from Group 1) takes our approaches approximately 27 and 37 minutes respectively, while the next best on accuracy models require approximately 15 hours (ERP+NN and DTW+NN, Table 2).

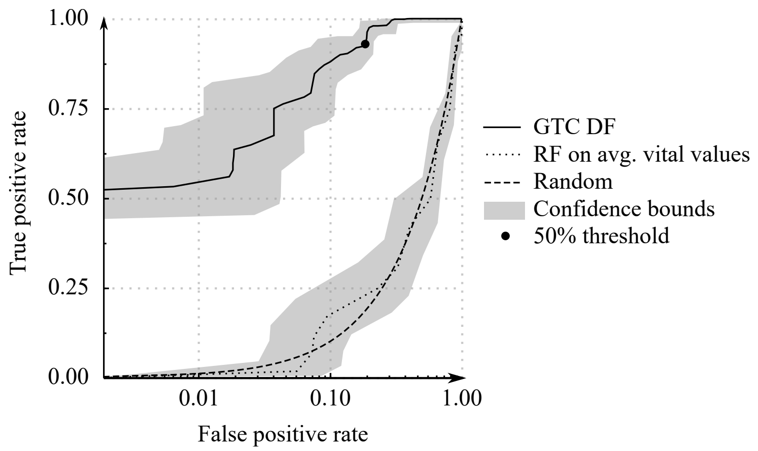

Figure 9: Receiver Operating Characteristic obtained for GTC-DF algorithm on the bleeding detection data set compared to the performance of the Random Forest algorithm on the flattened variant of the same data. False positive rate is scaled logarithmically.

Table 5: P-values of the Wilcoxon signed-rank test on the 41 UCR data sets and between each pair of the evaluated algorithms. Gray background is indicative of a positive significance of performances with a .05% error. A "+1NN" suffix has been removed from column labels for brevity.

Algorithm	GTC DF	GTC Set	ERP	DTW	DTWC	EDR	SVM	RF	ED	L1	LCSSC	LCSS	ED+5NN	Linf	ED+CVkNN	ED+10NN
GTC DF		6.6e-3	2.4e-3	1.5e-4	1.5e-4	1.7e-5	2.3e-4	5.7e-7	6.9e-6	9.7e-5	2.7e-5	2.8e-5	4.2e-7	2.0e-7	8.8e-8	5.4e-8
GTC Set	0.994		3.9e-3	3.0e-4	2.9e-4	2.4e-5	3.8e-4	4.4e-6	1.3e-5	1.3e-4	4.1e-5	4.5e-5	5.2e-7	2.8e-7	1.4e-7	8.8e-8
ERP+1NN	0.998	0.996		8.6e-4	2.2e-3	7.9e-5	8.0e-2	3.2e-2	2.7e-4	1.5e-4	8.5e-4	8.1e-4	6.5e-6	1.3e-5	2.4e-6	1.9e-6
DTW+1NN	1.000	1.000	0.999		0.819	1.8e-3	0.898	0.569	2.6e-2	5.4e-2	0.180	0.180	5.4e-5	1.1e-4	9.0e-6	6.5e-6
DTWC+1NN	1.000	1.000	0.998	0.292		1.7e-3	0.892	0.592	2.7e-2	7.1e-2	0.175	0.173	5.4e-5	7.5e-5	9.0e-6	6.5e-6
EDR+1NN	1.000	1.000	1.000	0.998	0.998		0.997	0.996	0.958	0.992	0.945	0.944	0.738	0.341	0.447	0.447
SVM	1.000	1.000	0.922	0.104	0.111	3.1e-3		0.104	2.2e-4	1.2e-2	2.5e-2	2.4e-2	4.0e-7	2.1e-6	3.0e-7	2.6e-7
RF	1.000	1.000	0.969	0.436	0.413	3.8e-3	0.898		2.9e-2	0.124	0.140	0.147	1.0e-5	4.8e-5	5.5e-7	3.4e-7
ED+1NN	1.000	1.000	1.000	0.975	0.973	4.4e-2	1.000	0.971		0.930	0.373	0.384	4.7e-7	2.4e-6	1.8e-7	1.2e-7
L1+1NN	1.000	1.000	1.000	0.951	0.935	8.3e-3	0.988	0.879	7.2e-2		0.288	0.291	7.7e-6	9.3e-6	2.6e-7	1.8e-7
LCSSC+1NN	1.000	1.000	0.999	0.823	0.829	5.6e-2	0.976	0.863	0.632	0.716		0.275	5.8e-2	9.2e-3	4.4e-3	4.0e-3
LCSS+1NN	1.000	1.000	0.999	0.823	0.830	5.8e-2	0.976	0.856	0.621	0.714	0.763		5.8e-2	9.3e-3	4.5e-3	4.1e-3
ED+5NN	1.000	1.000	1.000	1.000	1.000	0.266	1.000	1.000	1.000	1.000	0.944	0.944		3.4e-3	1.2e-6	4.2e-7
Linf+1NN	1.000	1.000	1.000	1.000	1.000	0.664	1.000	1.000	1.000	1.000	0.991	0.991	0.997		0.860	0.838
ED+CVkNN	1.000	1.000	1.000	1.000	1.000	0.559	1.000	1.000	1.000	1.000	0.996	0.996	1.000	0.143		0.500
ED+10NN	1.000	1.000	1.000	1.000	1.000	0.559	1.000	1.000	1.000	1.000	0.996	0.996	1.000	0.166	0.977	

7.7 Interpretability of Models

The ability to interpret a trained machine learning model typically improves understanding of the studied process, it may lead to useful discoveries, and it generally improves the acceptance of the model by its end-users. Many of the most powerful machine learning algorithms belong to the informal class of black (or opaque) box algorithms and specifically lack this useful ability. In our work, a single GTC is a graph of a usually small size (typically less than five tests, this number can however be controlled and further reduced if needed). The resulting complexity of a single GTC is therefore manageable and the model can practically be read by a typical trained user. However, the large amount and the redundancy of GTCs in large GTC-DF or a GTC-Set models may still make it difficult for the user to comprehend and interpret their structures. In this section, we present a two straightforward methods to extract a small but representative subset of interpretable GTCs from a GTC-Set model.

The first method is a non-weighed coverage algorithm guided by immediate information gain. At each step of the process, all GTCs are evaluated and the one with the highest information gain is selected. Next, all SSTSs correctly classified by this selected GTC are removed form data. This sequence is repeated until all SSTSs have been removed, or until no remaining GTC has a strictly positive information gain, or until a user-specified number of GTCs have been extracted. We refer to this method as the "Coverage selection method".

This method is similar in nature to the feature selection steps in CBA (Liu et al., 1998) and CMAR (Li et al., 2001) algorithms. However, while the CBA and the CMAR use feature selection to build a classifier from a pool of already extracted patterns, our algorithms use the method presented below to extract an interpretable and informative set of patterns from an already existing and functional classifier.

The application of p boolean patterns as a list of exception rules defines $p + 1$ combinations (e.g. the second rule is only tested if the first one does not apply). However, the independent application of p boolean patterns defines 2^p combinations. The second method is a greedy forward selection guided by the immediate information gain from all the considered patterns i.e. by the 2^p combinations. This second method is more likely to over fit than the first method when a large number of patterns is selected. But it gives an equal importance to all the patterns and observations. We refer to this method as the "Combination selection method".

The primary goal of the extracted patterns is not to perform predictions but to help the user interpret the models. As shown below, the selected GTCs typically show reduced classification performance but lower complexity than the corresponding full GTC-Sets.

Figure 10 shows the first two selected GTCs by the Combination selection method on the first cross-validation folds of a few UCR data sets (Coffee, CBF, ECG200, Wager, Yoga) and the Bleeding Detection Data Set. Figure 11 shows the empirical class distribution of the held-out test data classified by these top GTCs (the held-out test sets have not been used either for training or selection of the GTCs). We can see a very good effectiveness of just the first two (or just one for the Coffee data set) greedily selected GTCs at expressing output class distributions. For instance, in case of the CBF data set using the first selected GTC enables perfect separation of class 2 from the rest of the data, and adding the second greedily selected GTC discriminates class 1 from class 3 data in the remainder. Other results shown in Figure 11 indicate a very strong, even if not perfect, utility of just the top 2 GTCs to express class distributions in data. This suggests a potential for obtaining highly interpretable and simple models with impressive classification performance if that is attainable, and gradually adding complexity as required to achieve desired accuracy of classification while limiting overall complexity of the resulting models and maintaining their interpretability.

Figure 12 illustrates an example of application of the single top GTC extracted for the first SSTS of the first test fold of the UCR Coffee data set. The time series graph depicts the original scalar time series of the original data and the panel above it depicts occurrences of the discrete events extracted from it. This particular GTC requires that the standard deviation of the raw signal computed on a trailing time window 16 time units wide ought to peak-up (show a local maximum over time) during period between 226 and 252 time units from the time of occurrence of the starting event labeled as “begin”. This is the positive node plotted in the graph diagram in the right part of Figure 12. Concurrently, this GTC also requires that no event of the standard deviation of the raw time series computed over the trailing window 16 time units wide increase, crossing the threshold of 0.75 units, during time interval between 103 and 109 time units from “begin” (the negative node in the GTC diagram) will occur. If these conditions are met, the GTC is matched, and using just this GTC to perform classification of the underlying time series would be predicted as an instance of class 1.

Interestingly, the class distribution of the first fold of the Coffee data set can be explained perfectly with just a single GTC of a relatively small size (Fig. 6). It only consists of three tests (Fig. 10). We conclude that this data set appears to be quite simple to handle. The first fold of the CBF data set can be explained perfectly and entirely with just two GTCs. In the ECG200 data set, the top two GTCs can classify correctly 90% of the held-out test data. Yoga appears to be the most complex of the data sets considered in Fig. 10). The top two GTCs extracted from its fist cross-validation fold are significantly more complex than in the case of other data sets, with 10 tests each. These two GTCs can correctly classify 76% of the held-out data. Interestingly, this finding is somewhat intuitive since for all evaluated algorithms this data takes the longest to process due to its inherent complexity. For Yoga data set, the GTC models achieve prevailing accuracy but they require more GTCs of greater complexity to accomplish that.

Table 6 summarizes the aggregated classification performance obtained with the two selection methods, when varying the number of GTCs used per data set, and compared to the results obtained when using the complete GTC-Set. We use UCR Group 1 and Bleeding Detection Data Set. The results reflect average performance from 10-fold cross-validation, so the extracted GTCs may vary between folds. In terms of error rates, UCR:Trace, UCR:Lighting2, UCR:ECG200, UCR:Coffee and UCR:Beef data are are well handled by the top two GTCs in comparison to the fully developed GTC-Set. On the other hand, performance revealed on UCR:2Patterns and UCR:Synthetic data substantially diminishes when just the simple two-GTC models are used. Finally, The Combination selection method performs better that the Coverage selection method on most data sets (16 over 18 for two selected GTCs, and 14 over 18 for four selected GTCs).

8. Conclusion

We introduced Graphs of Temporal Constraints (GTC), a new expressive model for temporal pattern representation. We also presented two methods (GTC-DF and GTC-Set) of inferring GTCs from data to enable classification of Symbolic and Scalar Time Sequences (SSTS). Our methods stand-out from previously known approaches because: (1) They offer a high power of expression, enabled by the parametric and structural nature of the proposed representation; (2) The computational cost of learning and applying these models is manageable and often competitive when compared to the most potent alternatives; (3) The

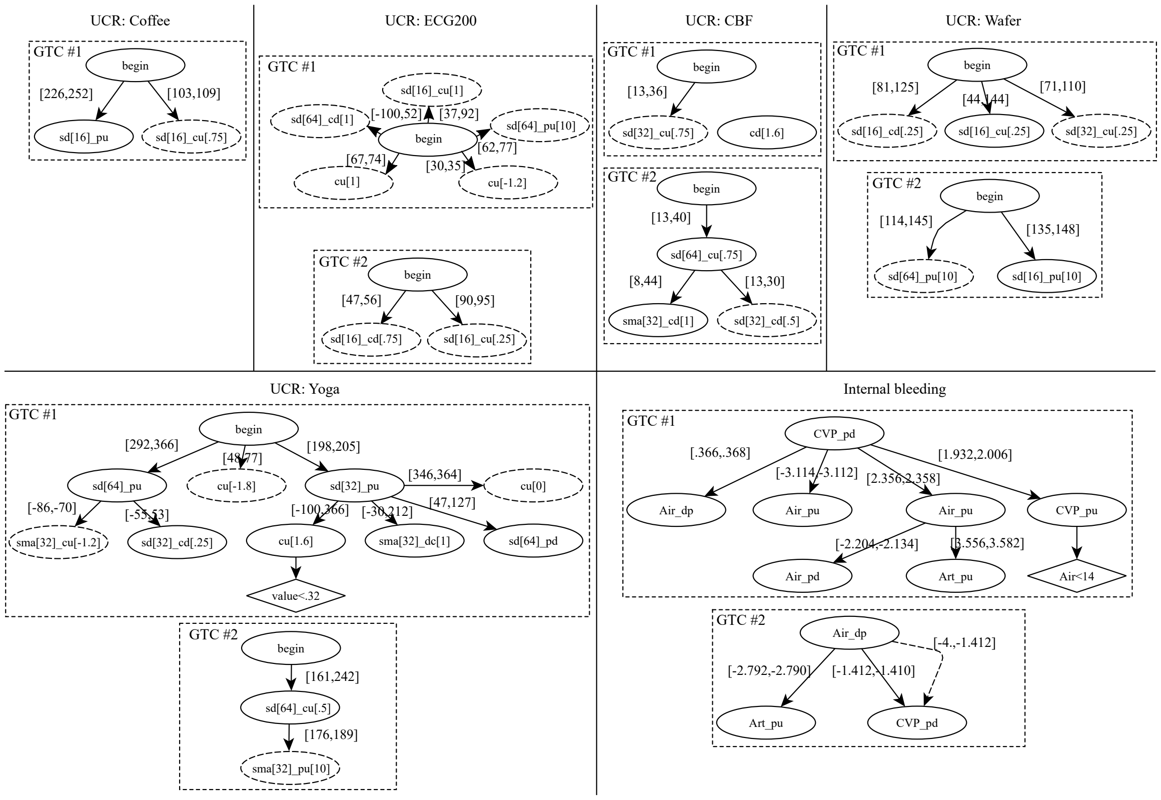

Figure 10: Graphical representations of the first two selected GTCs for the first cross-validation fold of a few evaluation data sets with the Combination selection method. Meaning of the event and scalar names: **begin**: begin of the SSTS, **sd[x]**: standard deviation over the trailing window x time units wide, **cd[x]**: signal crosses-down a threshold value x, **cu[x]**: signal crosses-up a threshold value x, **sma[x]**: simple moving average over the trailing window x time units wide, **pu**: peak up (local maximum over time), **pd**: peak down (local minimum over time), **CVP**: central venous pressure, **Air**: airway pressure, **Art**: arterial blood pressure.

users can read and interpret the models; and (4) In many cases, the users can easily project any new SSTS data and pursue its meaningful interpretation using only a handful of the most informative GTCs.

A wide range of experiments have been conducted to evaluate the proposed algorithms against a rich and diverse collection of benchmark data, and they have been compared to state-of-the-art alternative methods of temporal data classification. Experiments have shown that the proposed algorithms on average decisively outperform previously known best methods in terms accuracy of their predictions, while remaining highly competitive in terms of overall computational costs. Additionally, we have shown how easy it is to interpret the resulting models and we have presented a simple greedy procedure that in many cases yields a manageably small yet highly expressive and highly accurate models

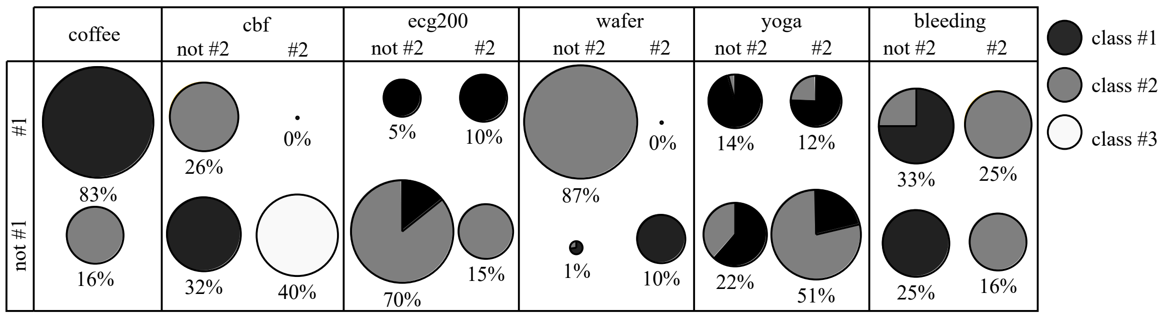

Figure 11: Held-out set empirical class separation achieved by simultaneously using the top two greedily selected GTCs for each of the considered data sets by the Combination selection method. For Coffee data set, only one GTC is needed to achieve the perfect class separation on the particular subset of testing data. The surface of each area represents the proportion of data it represents. This proportion is also shown with the percentage value beneath each graph. Pie charts are used to show distributions of target classes.

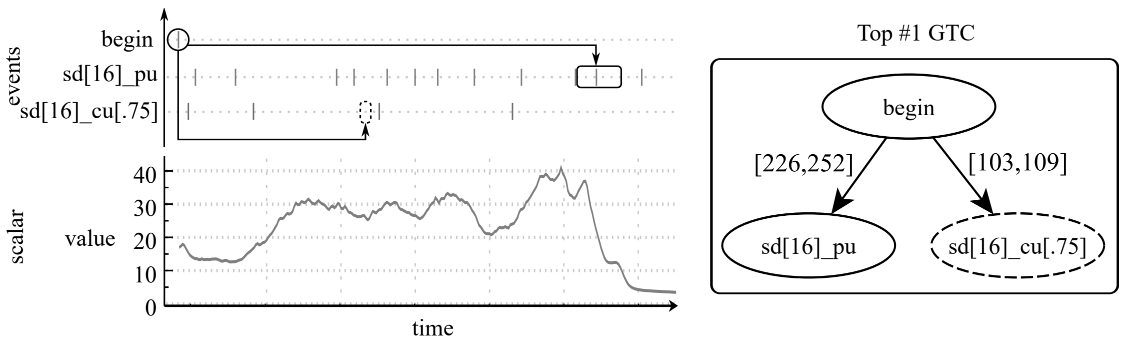

Figure 12: Instance of test SSTS of the UCR Coffee data set and illustration of the application of the first selected GTC extracted for it using the greedy procedure.

that can drive knowledge discovery and interpretability of the results in many real-world application scenarios.

Data Set	Classes	GTC Set	Top 2 Cov	Top 2 Cb	Cov/Cb	Gb/Orig	Top 4 Cov.	Top 4 Cb	Cov/Gb	Cb/Orig
Trace	5	**.000**	.325	**.000**		**.000**	.325	.005	65.000	
Lighting2	**2**	.223	.298	.289	1.029	1.296	.298	.248	1.200	**1.111**
ECG200	**2**	.120	.230	.190	1.211	1.583	.205	.175	1.171	1.458
Coffee	**2**	.036	.071	.071	1.000	2.000	.071	.071	1.000	2.000
Beef	6	.250	.683	.500	1.367	2.000	.567	.500	1.133	2.000
OSULeaf	7	.265	.520	.550	**.947**	2.077	.505	.419	1.205	1.581
Lighting7	7	.203	.566	.538	1.052	2.655	.469	.406	1.155	2.000
Wafer	**2**	.001	**.003**	.002	1.429	2.800	**.001**	**.002**	**.625**	3.200
50words	51	.235	.768	.754	1.019	3.202	.691	.625	1.104	2.657
CBF	4	.004	.014	.014	1.000	3.250	.013	.015	.857	3.500
Adiac	38	.256	.941	.930	1.012	3.630	.904	.816	1.108	3.185
Yoga	3	.045	.245	.222	1.102	4.946	.172	.198	.867	4.419
GunPoint	3	.010	.050	.050	1.000	5.000	.050	.055	.909	5.500
FaceFour	5	.018	.339	.098	3.455	5.500	.339	.116	2.923	6.500
Fish	8	.074	.700	.546	1.283	7.346	.500	.271	1.842	3.654
FaceAll	15	.045	.672	.684	.983	15.22	.557	.492	1.132	10.96
Synthetic	7	.012	.588	.478	1.230	41.00	.392	.143	2.733	12.28
2Patterns	5	.001	.301	.300	1.006	374.5	.224	.087	2.568	109.2

Table 6: Comparison of empirical classification error rates observed via 10-fold cross-validation when using only the top few (2 and 4) GTCs obtained using the Coverage (Cov) and Combination (Cb) selection methods, versus using the fully developed GTC-Set model. "Cb/Orig" denotes the ratio of error rates of the compact model extracted by the combination selection method vs. full GTC-Set. "Cov/Cb" denotes the ratio of error rates of the coverage selection method vs. the combination selection method. It is intended to reflect the drop of performance due to using a simplified representation. Entries are sorted by the ratio for the 2-GTC models ("Cb/Orig").

References

Rakesh Agrawal and Ramakrishnan Srikant. Fast algorithms for mining association rules in large databases. In *Proceedings of the 20th International Conference on Very Large Data Bases*, VLDB '94, pages 487–499, San Francisco, CA, USA, 1994. Morgan Kaufmann Publishers Inc. ISBN 1-55860-153-8. URL `http://dl.acm.org/citation.cfm?id=645920.672836`.

Johannes Aßfalg, Hans-Peter Kriegel, Peer Kröger, Peter Kunath, Alexey Pryakhin, and Matthias Renz. Similarity Search on Time Series Based on Threshold Queries. *Advances in Database Technology*, pages 276–294, 2006.

Iyad Batal, Dmitriy Fradkin, James Harrison, Fabian Moerchen, and Milos Hauskrecht. Mining recent temporal patterns for event detection in multivariate time series data. *Proceedings of the 18th ACM SIGKDD international conference on Knowledge discovery and data mining - KDD '12*, page 280, 2012.

Stephen D. Bay and Michael J. Pazzani. Detecting group differences: Mining contrast sets. *Data Mining and Knowledge Discovery*, 5(3):213–246, 2001. ISSN 1573-756X. doi: 10.1023/A:1011429418057. URL `http://dx.doi.org/10.1023/A:1011429418057`.

Donald Berndt and James Clifford. Using dynamic time warping to find patterns in time series. *Workshop on Knowledge Knowledge Discovery in Databases*, 398:359–370, 1994.

Leo Breiman. Random forests. *Machine learning*, pages 5–32, 2001.

Björn Bringmann, Siegfried Nijssen, and Albrecht Zimmermann. Pattern-based classification: A unifying perspective. *CoRR*, abs/1111.6191, 2011. URL `http://arxiv.org/abs/1111.6191`.

Lei Chen and Raymond Ng. On the marriage of Lp-norms and edit distance. *Proceedings of the 30th International Conference on Very Large Data Bases*, 30:792–803, 2004.

Lei Chen, M. Tamer Özsu, and Vincent Oria. Robust and fast similarity search for moving object trajectories. *Proceedings of the 2005 ACM SIGMOD international conference on Management of data - SIGMOD '05*, page 491, 2005.

Rina Dechter. Temporal constraint networks, 1991.

Janez Demšar. Statistical comparisons of classifiers over multiple data sets. *J. Mach. Learn. Res.*, 7:1–30, December 2006. ISSN 1532-4435.

Houtao Deng, George Runger, Eugene Tuv, and Martyanov Vladimir. A time series forest for classification and feature extraction. *Information Sciences*, 239:142–153, 2013.

Hui Ding, Goce Trajcevski, Peter Scheuermann, Xiaoyue Wang, and Eamonn Keogh. Querying and mining of time series data: experimental comparison of representations and distance measures. *Proceedings of the VLDB Endowment*, 1(2):1542–1552, 2008.

Guozhu Dong and Jinyan Li. Efficient mining of emerging patterns: Discovering trends and differences. In *Proceedings of the Fifth ACM SIGKDD International Conference on Knowledge Discovery and Data Mining*, KDD '99, pages 43–52, New York, NY, USA, 1999. ACM. ISBN 1-58113-143-7. doi: 10.1145/312129.312191. URL `http://doi.acm.org/10.1145/312129.312191`.

Christophe Dousson and Thang Vu Duong. Discovering chronicles with numerical time constraints from alarm logs for monitoring dynamic systems. *IJCAI International Joint Conference on Artificial Intelligence*, 1:620–626, 1999.

Elias Frentzos, Kostas Gratsias, and Yannis Theodoridis. Index-Based Most Similar Search. *Proceedings of the 23th International Conference on Data Engineering (ICDE'07)*, pages 816–825, 2007.

Yoav Freund and Robert E. Schapire. A Short Introduction to Boosting. 14(5):771–780, 2009.

Mathieu Guillame-Bert. Datasets for gtc classification. URL `http://mathieu.guillame-bert.com/dataset`.

Mathieu Guillame-Bert. *Learning Temporal Association Rules on Symbolic Time Sequences.* PhD thesis, 2012.

Mathieu Guillame-Bert and Artur Dubrawski. Learning Temporal Rules to Forecast Events in Multivariate Time Sequences. In *NIPS Workshop : Machine Learning for Clinical Data Analysis, Healthcare and Genomics*, 2014.

Jiawei Han, Jian Pei, Yiwen Yin, and Runying Mao. Mining frequent patterns without candidate generation: A frequent-pattern tree approach. *Data Min. Knowl. Discov.*, 8 (1):53–87, January 2004. ISSN 1384-5810. doi: 10.1023/B:DAMI.0000005258.31418.83. URL `http://dx.doi.org/10.1023/B:DAMI.0000005258.31418.83`.

Eamonn Keogh and Chotirat Ann Ratanamahatana. Exact indexing of dynamic time warping. *Knowl. Inf. Syst.*, 7(3):358–386, March 2005.

Willi Klösgen. Advances in knowledge discovery and data mining. chapter Explora: A Multipattern and Multistrategy Discovery Assistant, pages 249–271. American Association for Artificial Intelligence, Menlo Park, CA, USA, 1996. ISBN 0-262-56097-6. URL `http://dl.acm.org/citation.cfm?id=257938.257965`.

Wenmin Li, Jiawei Han, and Jian Pei. Cmar: accurate and efficient classification based on multiple class-association rules. In *Data Mining, 2001. ICDM 2001, Proceedings IEEE International Conference on*, pages 369–376, 2001.

Bing Liu, Wynne Hsu, and Yiming Ma. Integrating classification and association rule mining. pages 80–86, 1998.

Heikki Mannila, Hannu Toivonen, and Inkeri Verkamo. Discovery of frequent episodes in event sequences. *Data Mining and Knowledge*, 289:259–289, 1997.

David Meyer, Friedrich Leisch, and Kurt Hornik. The support vector machine under test. *Neurocomputing*, 55(1-2):169–186, 2003.

Michael D. Morse and Jignesh M. Patel. An efficient and accurate method for evaluating time series similarity. *ACM SIGMOD international conference on Management of data*, page 569, 2007.

Stephen Muggleton. Inductive logic programming. *New Generation Computing*, 8(4):295–318, 1991.

Petra Kralj Novak, Nada Lavrač, and Geoffrey I. Webb. Supervised descriptive rule discovery: A unifying survey of contrast set, emerging pattern and subgroup mining. *J. Mach. Learn. Res.*, 10:377–403, June 2009. ISSN 1532-4435. URL `http://dl.acm.org/citation.cfm?id=1577069.1577083`.

S. Nowozin, K. Tsuda, T. Uno, T. Kudo, and G. Bakir. Weighted substructure mining for image analysis. In *2007 IEEE Conference on Computer Vision and Pattern Recognition*, pages 1–8, June 2007. doi: 10.1109/CVPR.2007.383171.

Jian Pei, Jiawei Han, B. Mortazavi-Asl, H. Pinto, Qiming Chen, U. Dayal, and Mei-Chun Hsu. Prefixspan,: mining sequential patterns efficiently by prefix-projected pattern growth. In *Data Engineering, 2001. Proceedings. 17th International Conference on*, pages 215–224, 2001. doi: 10.1109/ICDE.2001.914830.

J Ross Quinlan. *C4.5: Programs for Machine Learning*. Morgan Kaufmann Publishers Inc., San Francisco, CA, USA, 1993.

Juan J. Rodríguez and Carlos J. Alonso. Interval and dynamic time warping-based decision trees. *Proceedings of the 2004 ACM symposium on Applied computing - SAC '04*, page 548, 2004.

Juan J. Rodriguez, Carlos J. Alonso, and Henrik Bostrom. Learning first order logic time series classifiers: Rules and boosting. In DjamelA. Zighed, Jan Komorowski, and Jan Zytkow, editors, *Principles of Data Mining and Knowledge Discovery*, volume 1910 of *Lecture Notes in Computer Science*, pages 299–308. Springer Berlin Heidelberg, 2000.

Ramakrishnan Srikant and Rakesh Agrawal. Mining sequential patterns: Generalizations and performance improvements. In *Proceedings of the 5th International Conference on Extending Database Technology: Advances in Database Technology*, EDBT '96, pages 3–17, London, UK, UK, 1996. Springer-Verlag. ISBN 3-540-61057-X. URL `http://dl.acm.org/citation.cfm?id=645337.650382`.

M. Vlachos, G. Kollios, and D. Gunopulos. Discovering similar multidimensional trajectories. *Proceedings 18th International Conference on Data Engineering*, 2002.

Xifeng Yan, Hong Cheng, Jiawei Han, and Philip S. Yu. Mining significant graph patterns by leap search. In *Proceedings of the 2008 ACM SIGMOD International Conference on Management of Data*, SIGMOD '08, pages 433–444, New York, NY, USA, 2008. ACM. ISBN 978-1-60558-102-6. doi: 10.1145/1376616.1376662. URL `http://doi.acm.org/10.1145/1376616.1376662`.

Lexiang Ye and Eamonn Keogh. Time series shapelets: a new primitive for data mining. *Proceedings of the 15th ACM SIGKDD international conference on Knowledge discovery and data mining*, pages 947–956, 2009.

Mohammed J. Zaki. SPADE: An efficient algorithm for mining frequent sequences. *Machine Learning*, 42(1-2):31–60, 2001.